Reduced order surrogate modeling technique for linear dynamic systems

Vahid Yaghoubi, Sadegh Rahrovani, Hassan Nahvi, Stefano Marelli

ETH zürich

Reduced order surrogate modeling technique for linear dynamic systems

V. Yaghoubi, S. Rahrovani, H. Nahvi, S. Marelli

Chair of Risk, Safety and Uncertainty Quantification
Stefano-Franscini-Platz 5
CH-8093 Zürich

Risk, Safety & Uncertainty Quantification

Data Sheet

Journal:	Mechanical Systems and Signal Processing
Report Ref.:	RSUQ-2018-002
Arxiv Ref.:	–
DOI:	https://doi.org/10.1016/j.ymssp.2018.02.020
Date submitted:	7 May 2017
Date accepted:	10 February 2018

Reduced order surrogate modeling technique for linear dynamic systems

Vahid Yaghoubi, Sadegh Rahrovani, Hassan Nahvi, Stefano Marelli

June 9, 2018

Abstract

The availability of reduced order models can greatly decrease the computational costs needed for modeling, identification and design of real-world structural systems. However, since these systems are usually employed with some uncertain parameters, the approximant must provide a good accuracy for a range of stochastic parameters variations. The derivation of such reduced order models are addressed in this paper. The proposed method consists of a polynomial chaos expansion (PCE)-based state-space model together with a PCE-based modal dominancy analysis to reduce the model order. To solve the issue of spatial aliasing during mode tracking step, a new correlation metric is utilized. The performance of the presented method is validated through four illustrative benchmarks: a simple mass-spring system with four Degrees Of Freedom (DOF), a 2-DOF system exhibiting a mode veering phenomenon, a 6-DOF system with large parameter space and a cantilever Timoshenko beam resembling large-scale systems.

1 Introduction

Modeling and simulation (M&S) play important roles in the analysis, design, and optimization of engineering systems. M&S targets deriving models with enough accuracy for their intended purpose. These models can be used to predict the systems' response under different loading and environmental conditions. Although the development of computational power of modern computers has been very fast in recent years, more precise description of model properties and more detailed representation of the system geometry still result in large-scale, more complex models of dynamical systems with considerable execution time and memory usage. Model reduction Antoulas et al. (2001), efficient simulation Yaghoubi et al. (2016); Avitabile and O'Callahan (2009); Liu et al. (2012) and parallel simulation methods Yaghoubi et al. (2015); Tak and Park (2013) are different strategies to address this issue.

Nowadays, due to an ever increasing need for accurate and robust prediction of systems' response, engineering models are almost always employed with some parameters to allow variations in material properties, geometries, initial and boundary conditions. Consequently, numerous model evaluations are normally required for the procedure of modeling, identification and design of real-world applications in order to optimize the models' performance. This can be prohibitively expensive for computationally demanding models. In the literature, several approaches address this issue by replacing such models with approximations that can reproduce the essential features faster, *e.g.* surrogate modeling Frangos et al. (2010) and parametric model order reduction (PMOR) Benner et al. (2013).

Surrogate models can be created intrusively or non-intrusively. In intrusive approaches, the equations of a system are modified such that one explicit function relates the stochastic properties of the system responses to the random inputs. The perturbation method Schuëller and Pradlwarter (2009) is a classical tool used for this purpose but it is only accurate when the random inputs have small coefficients of variation (COV). An alternative method is intrusive Polynomial Chaos Expansion (PCE) Ghanem and Spanos (2003). It was first introduced for Gaussian input random variables Wiener (1938) and then extended to the other types of random variables leading to generalized polynomial chaos Xiu and Karniadakis (2002); Soize and Ghanem (2004). In non-intrusive approaches, already existing deterministic codes are evaluated at several sample points selected over the parameter space. This selection depends on the methods employed to build the surrogate model, namely regression Blatman and Sudret (2010); Berveiller et al. (2006) or projection methods Gilli et al. (2013); Knio et al. (2001). Kriging Fricker et al. (2011); Jones et al. (1998) and non-intrusive PCE Blatman and Sudret (2011) or combination thereof Kersaudy et al. (2015); Schöbi et al. (2015) are examples of the non-intrusive approaches. The major drawback of PCE methods, both intrusive and non-intrusive, is the large number of unknown coefficients in problems with large parameter spaces, which is referred to as the curse of dimensionality Sudret (2007). Sparse Blatman and Sudret (2008) and adaptive sparse Blatman and Sudret (2011) polynomial chaos expansions have been developed to tackle this issue.

Parametric model order reduction (PMOR) methods are analogous to regression-based non-intrusive surrogate modeling except that in PMOR, interpolations are performed not only on system responses Baur et al. (2011), like surrogate modeling Yaghoubi et al. (2017), but also on the reduced bases Amsallem and Farhat (2008) and reduced models Amsallem and Farhat (2011); Panzer et al. (2010) evaluated over the parameter space. In this regard, some attempts have been made recently to surrogate the models as well, e.g. the modal models Manan and Cooper (2010); Dertimanis et al. (2017), NARX models Mai et al. (2016) and time-varying ARMA models Bogoevska et al. (2017). However, they were only applied to very small cases with single excitation and single sensor location, known as single-input, single-output (SISO) systems. Since the extension of the modal models to nonlinear systems

is not straightforward and NARX models become very complex for structures with Multi-input, Multi-output (MIMO), they are not a suitable model for real life applications.

State-space (SS) is the most common model for dynamic systems due to the following reasons: (i) it can represent MIMO systems as convenient as SISO systems, (ii) it can easily be expanded to the more complex physical phenomena such as nonlinear systems, time-varying systems, etc. Unlike PMOR methods which are mostly developed for SS models Benner et al. (2013), there is a lack of literature in surrogating these models. Moreover, complex dynamic systems have large model orders, therefore applying PCE directly on these models may not be feasible. An appropriate approach could be to construct surrogate models jointly with a proper model reduction method which is at the focus of this paper. It opens up a new field which requires more investigation.

In Yang et al. (2015), Yang *et al.* combine intrusive PCE with a projection based model reduction method and applied them to uncertain structures. In Kim (2015), Kim developed a reduced order modeling technique for parametric linear systems. In this method, Karhunen-Loeve approach is used in frequency domain to calculate optimal modes subject to the simultaneous excitations. The method has been successfully applied to a structural systems and later in Kim (2016), was extended to aeroelastic systems.

The main contribution of this paper is developing a reduced-order PCE-based surrogate model for linear dynamic systems when they are presented in SS form. For this purpose, the PCE-based surrogate model is developed in conjunction with modal dominancy analysis Rahrovani et al. (2014) in order to reduce the model order, if required, while preserving the model structure. Computational efficiency is another beneficial feature of the modal dominancy analysis which is of our special interest in this work. The proposed method is organized around two steps. In the first step, the modes are transformed to have similar orientations to those of a reference model and in the second step, interpolation is performed using PCE. The other novelties of the paper are: (i) new correlation metric to track system modes when small number of sensors are available, (ii): QR-factorization is employed to treat the well-known problem of non-unique eigenvectors of coalescent modes.

The outline of the paper is as follows. In Section 2, the problem is formulated and in Section 4, after a short review of the pertinent materials from linear system theories and polynomial chaos expansion, the proposed methodology is elaborated. In Section 5, the method is applied to several academic case studies resembling challenges in the structures.

2 Problem formulation

Consider the spatially-discretized governing second-order equation of motion of a linear time-invariant (LTI) system as

$$\begin{aligned} \boldsymbol{M}(\boldsymbol{x})\ddot{\boldsymbol{q}}(t) + \boldsymbol{V}(\boldsymbol{x})\dot{\boldsymbol{q}}(t) + \boldsymbol{K}(\boldsymbol{x})\boldsymbol{q}(t) &= \boldsymbol{f}(t) \\ \boldsymbol{y}(t) &= \boldsymbol{C}'(\boldsymbol{x})\boldsymbol{q}(t) \end{aligned} \tag{1}$$

in which for an N-DOF system with n_u system inputs and n_y system outputs, $\boldsymbol{q}(t) \in \mathbb{R}^N$ is the displacement vector, $\boldsymbol{y}(t) \in \mathbb{R}^{n_y}$ is the system output, $\boldsymbol{f}(t)$ is the external load vector which is governed by a transformation of stimuli vector $\boldsymbol{f}(t) = \boldsymbol{P_u}\boldsymbol{u}(t)$; with $\boldsymbol{u}(t) \in \mathbb{R}^{n_u}$. $\boldsymbol{x} \in \mathbb{R}^{n_x}$ is the parameter vector and real positive-definite symmetric matrices $\boldsymbol{M}, \boldsymbol{V}, \boldsymbol{K} \in \mathbb{R}^{N\times N}$ are mass, damping and stiffness matrices, respectively. The output matrix $\boldsymbol{C}' \in \mathbb{C}^{n_y \times N}$, maps the displacement vector to the output $\boldsymbol{y}(t)$.

The SS realization of the equation of motion in Eq. (1) can be written as

$$\begin{aligned} \dot{\boldsymbol{\eta}}(t) &= \boldsymbol{A}(\boldsymbol{x})\boldsymbol{\eta}(t) + \boldsymbol{B}(\boldsymbol{x})\boldsymbol{u}(t) \\ \boldsymbol{y}(t) &= \boldsymbol{C}(\boldsymbol{x})\boldsymbol{\eta}(t) + \boldsymbol{D}(\boldsymbol{x})\boldsymbol{u}(t) \end{aligned} \tag{2}$$

where $\boldsymbol{A} \in \mathbb{C}^{2N\times 2N}$, $\boldsymbol{B} \in \mathbb{C}^{2N\times n_u}$, $\boldsymbol{C} \in \mathbb{C}^{n_y\times 2N}$, and $\boldsymbol{D} \in \mathbb{C}^{n_y\times n_u}$. $\boldsymbol{\eta}(t) = [\boldsymbol{q}(t)^T, \dot{\boldsymbol{q}}^T(t)]^T \in \mathbb{R}^{2N}$ is the state vector. $\boldsymbol{A}$ and $\boldsymbol{B}$ are related to mass, damping and stiffness as follows

$$\boldsymbol{A} = \begin{bmatrix} \boldsymbol{0} & \boldsymbol{I} \\ -\boldsymbol{M}^{-1}\boldsymbol{V} & -\boldsymbol{M}^{-1}\boldsymbol{K} \end{bmatrix}, \boldsymbol{B} = \begin{bmatrix} \boldsymbol{0} \\ \boldsymbol{M}^{-1}\boldsymbol{P}_u \end{bmatrix}. \tag{3}$$

The output matrix $\boldsymbol{C}$ maps the states to the output $\boldsymbol{y}$ and $\boldsymbol{D}$ is the associated direct throughput matrix. Such system with order of $2N$ is denoted by

$$\boldsymbol{\Sigma}(\boldsymbol{x}) = \{\boldsymbol{A}(\boldsymbol{x}), \boldsymbol{B}(\boldsymbol{x}), \boldsymbol{C}(\boldsymbol{x}), \boldsymbol{D}(\boldsymbol{x})\} \in O(2N).$$

In cases with large model orders, one can use model reduction methods to reduce the model order to $2n \ll 2N$ while retaining the main properties of the full model. For this purpose, several methods have been proposed in the literature which have been comprehensively reviewed in Antoulas et al. (2001). One of these approaches is modal dominancy analysis based on modal contributions Rahrovani et al. (2014) which is discussed more in Section 4.2. In this case, the reduced model $\{\boldsymbol{\Sigma}_r\} = \{\boldsymbol{A}_r(\boldsymbol{x}), \boldsymbol{B}_r(\boldsymbol{x}), \boldsymbol{C}_r(\boldsymbol{x}), \boldsymbol{D}_r(\boldsymbol{x})\} \in O(2n)$ can be presented as

$$\begin{aligned} \dot{\boldsymbol{\eta}}_r(t) &= \boldsymbol{A}_r(\boldsymbol{x})\boldsymbol{\eta}_r(t) + \boldsymbol{B}_r(\boldsymbol{x})\boldsymbol{u}(t) \\ \boldsymbol{y}(t) &= \boldsymbol{C}_r(\boldsymbol{x})\boldsymbol{\eta}_r(t) + \boldsymbol{D}_r(\boldsymbol{x})\boldsymbol{u}(t) \end{aligned} \tag{4}$$

with $\boldsymbol{\eta}_r(t) \in \mathbb{R}^{2n}$.

The problem is then as follows

Given $\{\boldsymbol{\Sigma}^{(k)}\}_{k=1}^{N_{ED}} = \{\boldsymbol{\Sigma}(\boldsymbol{x}^{(k)})\}_{k=1}^{N_{ED}}$ denoting systems evaluated at N_{ED} points sampled from the parameter space $\boldsymbol{x}$. The systems are assumed to be minimally realized linear time-invariant(LTI) with equal number of states at all different realizations. Furthermore, let $\boldsymbol{x}^{(0)} \neq \boldsymbol{x}^{(k)}, \quad k = 1, 2, ..., N_{ED}$ be a new parameter set from the parameter space.

Find a method which can approximate $\boldsymbol{\Sigma}_r(\boldsymbol{x}^{(0)})$ by making PCEs over the already evaluated systems $\{\boldsymbol{\Sigma}^{(k)}\}_{k=1}^{N_{ED}}$.

3 Background

This section briefly reviews some features from linear system theories and polynomial chaos expansions pertinent to the proposed method.

3.1 Linear system theories

In system theory, realization of an SS model is not unique. That is, given an input-output relationship, a realization of an SS model is any quadruple of $\{\boldsymbol{A}, \boldsymbol{B}, \boldsymbol{C}, \boldsymbol{D}\}$[1] such that $[\boldsymbol{u}(t), \boldsymbol{y}(t)]$ describes the input and output. Obviously, there are infinite number of realizations for an SS model which are called equivalent systems. They are defined as follows,

Definition 1. *Let $\boldsymbol{\Sigma} \in O(2N)$ be a system in SS representation, $\boldsymbol{T} \in \mathbb{R}^{2N\times 2N}$ be a nonsingular matrix and $\boldsymbol{\eta} = \boldsymbol{T}\boldsymbol{\eta}_e$. Then, the model $\boldsymbol{\Sigma}_e = \boldsymbol{T}(\boldsymbol{\Sigma}) \in O(2N)$*

$$\begin{aligned} \dot{\boldsymbol{\eta}}_e(t) &= \boldsymbol{A}_e\boldsymbol{\eta}_e(t) + \boldsymbol{B}_e\boldsymbol{u}(t) \\ \boldsymbol{y}_e(t) &= \boldsymbol{C}_e\boldsymbol{\eta}_e(t) + \boldsymbol{D}_e\boldsymbol{u}(t) \end{aligned} \tag{5}$$

where

$$\boldsymbol{A}_e = \boldsymbol{T}^{-1}\boldsymbol{A}\boldsymbol{T}, \boldsymbol{B}_e = \boldsymbol{T}^{-1}\boldsymbol{B}, \boldsymbol{C}_e = \boldsymbol{C}\boldsymbol{T}, \boldsymbol{D}_e = \boldsymbol{D} \tag{6}$$

is said to be (algebraically) equivalent to $\boldsymbol{\Sigma}$ and $\boldsymbol{T}$ is called equivalence transformation.

A common SS realization is the modal realization which is discussed in the subsequent section.

Modal realization

Assume that the dynamical system $\boldsymbol{\Sigma} \in O(2N)$ is diagonalizable and let $\boldsymbol{A}$ be a Hermitian matrix with the eigenvalue set of $\boldsymbol{\lambda} = \{\lambda_1, \lambda_2, ..., \lambda_{2N}\}$ and the corresponding eigenvector matrix $\boldsymbol{\Phi} = \{\boldsymbol{\phi}_1, \boldsymbol{\phi}_2, ..., \boldsymbol{\phi}_{2N}\}$. Using the transformation $\boldsymbol{T} = \boldsymbol{\Phi}$ the dynamical system $\boldsymbol{\Sigma}$ can be projected onto modal coordinates in the form of the following quadruple,

$$\bar{\boldsymbol{\Sigma}} = \boldsymbol{\Phi}(\boldsymbol{\Sigma}) = \{\bar{\boldsymbol{A}}, \bar{\boldsymbol{B}}, \bar{\boldsymbol{C}}, \boldsymbol{D}\} = \{\boldsymbol{\Phi}^{-1}\boldsymbol{A}\boldsymbol{\Phi}, \boldsymbol{\Phi}^{-1}\boldsymbol{B}, \boldsymbol{C}\boldsymbol{\Phi}, \boldsymbol{D}\} \tag{7}$$

where $\bar{\boldsymbol{A}} = \boldsymbol{\Lambda} = diag(\lambda_1, \lambda_2, ..., \lambda_{2N})$, $\bar{\boldsymbol{B}} = [\bar{b}_1, \bar{b}_2, ..., \bar{b}_{2N}]$ is the modally projected input matrix, and $\bar{\boldsymbol{C}}=[\bar{c}_1, \bar{c}_2, ..., \bar{c}_{2N}]$ is the modally projected output matrix. In particular, it should be noted that the i^{th} column of $\bar{\boldsymbol{C}}$ is the projection of the i^{th} eigenvector of $\boldsymbol{A}$ to the space spanned by the output $\boldsymbol{y}$.

3.2 Polynomial chaos expansion

Let $\mathcal{M}$ be a computational model with n_x random inputs $\boldsymbol{X}=\{X_1, X_2, ..., X_{n_x}\}^{\mathrm{T}}$ and one output Y. Assume that the random variables are independent and thus, their joint probability distribution function (PDF) defined in the probability space $(\Omega, \mathscr{F}, \mathbb{P})$ is $f_{\boldsymbol{X}}(\boldsymbol{x}) =$

[1] The dependency of the system matrices on parameters $\boldsymbol{x}$ has been dropped for simplicity

$\prod_{i=1}^{n_x} f_{X_i}(x_i)$. Further, the system response $Y = \mathcal{M}(\boldsymbol{X})$ is assumed to be a second-order random variable, *i.e.* $\mathbb{E}\left[Y^2\right] < +\infty$ and belongs to the Hilbert space $\mathscr{H} = \mathscr{L}^2_{f_{\boldsymbol{X}}}(\mathbb{R}^{n_x}, \mathbb{R})$ of $f_{\boldsymbol{X}}$-square integrable functions of $\boldsymbol{X}$ with respect to the inner product:

$$\mathbb{E}\left[\psi(\boldsymbol{X})\phi(\boldsymbol{X})\right] = \int_{\mathcal{D}_{\boldsymbol{X}}} \psi(\boldsymbol{x})\phi(\boldsymbol{x}) f_{\boldsymbol{X}}(\boldsymbol{x}) \mathrm{d}\boldsymbol{x} \tag{8}$$

where $\mathcal{D}_{\boldsymbol{X}}$ is the support of $\boldsymbol{X}$. In order to make polynomial chaos expansion for Y, let us define multi-index set $\boldsymbol{\alpha} = (\alpha_1, \alpha_2, ..., \alpha_{n_x})$ to which, any multivariate polynomials can be constructed by

$$\psi_{\boldsymbol{\alpha}}(\boldsymbol{X}) = \prod_{i=1}^{n_x} \psi^{(i)}_{\alpha_i}(X_i)$$

where $\{\psi^{(i)}_{\alpha_i}(X_i), \alpha_i \in N\}$ is a univariate orthonormal polynomials defined with respect to the marginal PDFs. For instance, if the inputs are standard normal or uniform variables, the corresponding univariate polynomials are Hermite or Legendre polynomials, respectively. The multivariate polynomials in the input vector $\boldsymbol{X}$ are orthonormal with respect to the joint PDF $f_{\boldsymbol{X}}(\boldsymbol{x})$, *i.e.* :

$$\mathbb{E}\left[\psi_{\boldsymbol{\alpha}}(\boldsymbol{X})\psi_{\boldsymbol{\beta}}(\boldsymbol{X})\right] = \int_{\mathcal{D}_{\boldsymbol{X}}} \psi_{\boldsymbol{\alpha}}(\boldsymbol{x})\psi_{\boldsymbol{\beta}}(\boldsymbol{x}) f_{\boldsymbol{X}}(\boldsymbol{x}) \mathrm{d}\boldsymbol{x} = \delta_{\boldsymbol{\alpha}\boldsymbol{\beta}} \tag{9}$$

where $\delta_{\boldsymbol{\alpha}\boldsymbol{\beta}}$ is the Kronecker delta.

With these notations, the generalized polynomial chaos representation of Y reads Xiu and Karniadakis (2002):

$$Y = \sum_{\boldsymbol{\alpha} \in \mathbb{N}^{n_x}} \tilde{u}_{\boldsymbol{\alpha}} \psi_{\boldsymbol{\alpha}}(\boldsymbol{X}) \tag{10}$$

in which $\tilde{u}_{\boldsymbol{\alpha}}$ is a set of unknown deterministic coefficients which can be estimated non-intrusively by projection Ghanem and Ghiocel (1998); Ghiocel and Ghanem (2002) or least square regression methods Blatman and Sudret (2010); Berveiller et al. (2006). The latter is of interest here and will be briefly explained later on.

Prior to that, the infinite series in Eq.(10) has to be truncated. One approach is the Standard truncation scheme which include all polynomials corresponding to the set $\mathcal{A}^{n_x,p} = \{\boldsymbol{\alpha} \in \mathbb{N}^{n_x} \ : \ |\boldsymbol{\alpha}| \leq p\}$, where p is a maximum polynomial degree and $|\boldsymbol{\alpha}| = \sum_{i=1}^{n_x} \alpha_i$ is the total degree of polynomial $\psi_{\boldsymbol{\alpha}}$. The main drawback of this approach is rapid increase in the cardinality of the set $\mathcal{A}^{n_x,p} = \binom{n_x+p}{p} = P$ by increasing the number of parameters n_x and the order of polynomials p. However, in order to control it, suitable truncation strategies such as q-norm hyperbolic truncation Blatman and Sudret (2010) have been developed that drastically reduce the number of unknowns when n_x is large.

In order to estimate $\tilde{u}_{\boldsymbol{\alpha}}$ by least square regression, the truncation error ϵ is minimized via least square as follows:

$$Y = \mathcal{M}(\boldsymbol{X}) = \sum_{\boldsymbol{\alpha} \in \mathcal{A}^{n_x,p}} \tilde{u}_{\boldsymbol{\alpha}}\, \psi_{\boldsymbol{\alpha}}(\boldsymbol{X}) + \epsilon \equiv \tilde{\boldsymbol{U}}^{\mathrm{T}} \boldsymbol{\Psi}(\boldsymbol{X}) + \boldsymbol{\epsilon} \tag{11}$$

To formulate this procedure, let $\boldsymbol{\mathcal{X}} = \{\boldsymbol{x}^{(1)}, \boldsymbol{x}^{(2)}, ..., \boldsymbol{x}^{(N_{ED})}\}$ be an experimental design with N_{ED} space-filling samples of $\boldsymbol{X}$ and $\boldsymbol{\mathcal{Y}} = \{y^{(1)} = \mathcal{M}(\boldsymbol{x}^{(1)}), y^{(2)} = \mathcal{M}(\boldsymbol{x}^{(2)}), ..., y^{(N_{ED})} = \mathcal{M}(\boldsymbol{x}^{(N_{ED})})\}$ be their associated system responses. Then, the minimization problem is

$$\hat{\tilde{\boldsymbol{U}}} = \arg\min \mathbb{E}\left[\left(\tilde{\boldsymbol{U}}^{\mathrm{T}}\boldsymbol{\Psi}(\boldsymbol{X}) - \mathcal{M}(\boldsymbol{X})\right)^2\right]. \tag{12}$$

which admits a closed form solution as

$$\hat{\tilde{\boldsymbol{U}}} = (\boldsymbol{\Psi}^{\mathrm{T}}\boldsymbol{\Psi})^{-1}\boldsymbol{\Psi}^{\mathrm{T}}\boldsymbol{\mathcal{Y}}. \tag{13}$$

Here $\boldsymbol{\Psi}$ is the matrix containing the evaluations of the Hilbertian bases, that is $\boldsymbol{\Psi}_{ij} = \psi_{\boldsymbol{\alpha}_j}(\boldsymbol{x}^{(i)}), i = 1, 2, ..., N_{ED}, j = 1, 2, ..., P$.

The accuracy of PCE will be improved by reducing the effect of over-fitting in least square regression. This can be carried out by using sparse adaptive regression algorithms proposed in Hastie et al. (2007); Efron et al. (2004). In particular, the Least Angle Regression (LAR) algorithm has been demonstrated to be effective in the context of PCE by Blatman and Sudret Blatman and Sudret (2011). Readers interested to know more about calculating the PCE are referred to Marelli and Sudret (2015).

Vector-valued response

In the case of vector-valued response, *i.e.* $\boldsymbol{Y} \in \mathbb{R}^{N_Y}, N_Y > 1$, one can apply the presented approach componentwise. For models with large number of random outputs, this can make the algorithm computationally intractable. To avoid that, one can extract the main statistical features of the vectorial random response by principal component analysis (PCA). The concept has been adapted to the context of PCE by Blatman and Sudret Blatman and Sudret (2013).

Let us perform sample-based PCA by rewriting the $\boldsymbol{\mathcal{Y}}$ as the combination of its mean $\bar{\boldsymbol{\mathcal{Y}}}$ and covariance matrix as follows:

$$\boldsymbol{\mathcal{Y}} = \bar{\boldsymbol{\mathcal{Y}}} + \sum_{i=1}^{N_Y} \boldsymbol{u}_i \boldsymbol{v}_i^{\mathrm{T}} \tag{14}$$

where the $\boldsymbol{v}_i$'s are the eigenvectors of the covariance matrix:

$$COV(\boldsymbol{\mathcal{Y}}) = \mathbb{E}\left[(\boldsymbol{\mathcal{Y}} - \bar{\boldsymbol{\mathcal{Y}}})^{\mathrm{T}}(\boldsymbol{\mathcal{Y}} - \bar{\boldsymbol{\mathcal{Y}}})\right] = [\boldsymbol{v}_1, ..., \boldsymbol{v}_{N_Y}] \begin{bmatrix} l_1 & \dots & 0 \\ & \ddots & \\ 0 & \dots & l_{N_Y} \end{bmatrix} \begin{bmatrix} \boldsymbol{v}_1^{\mathrm{T}} \\ \vdots \\ \boldsymbol{v}_{N_Y}^{\mathrm{T}} \end{bmatrix}^{\mathrm{T}} \tag{15}$$

and the $\boldsymbol{u}_i$'s are vectors such that

$$\boldsymbol{u}_i = (\boldsymbol{\mathcal{Y}} - \bar{\boldsymbol{\mathcal{Y}}})\boldsymbol{v}_i. \tag{16}$$

Then, $\boldsymbol{\mathcal{Y}}$ can be approximated by the $\hat{N}_Y$-term truncation:

$$\boldsymbol{\mathcal{Y}} = \bar{\boldsymbol{\mathcal{Y}}} + \sum_{i=1}^{\hat{N}_Y} \boldsymbol{u}_i \boldsymbol{v}_i^{\mathrm{T}}, \quad \hat{N}_Y \ll N_Y. \tag{17}$$

Since $\bar{\boldsymbol{\mathcal{Y}}}$ and $\boldsymbol{v}_i^{\mathrm{T}}$ are the mean and the eigenvectors of the system responses, respectively; they are independent of the realization. Therefore, PC expansion can be applied directly on the $\hat{N}_Y \ll N_Y$ auxiliary variables $\boldsymbol{u}_i$. Besides, acknowledging the fact that the PCA is an invertible transform, the original output can be retrieved directly from Eq. (17) for every new prediction of $\boldsymbol{u}$.

4 Methodology

This section elaborate the proposed methodology to develop the reduced order PCE-based surrogate model for linear dynamic system. It consists of three major steps: (*i*) Tracking the eigensolution of a system while its parameters are varying, (*ii*) Ranking the modes based on their contribution to the input/output relation (*iii*) Making PCE-based surrogate model.

4.1 Correlation-based mode tracking

Mode tracking is an approach applicable to eigenvalue problems with variable parameters in order to maintain correspondence between reference and perturbed eigensolutions. For this purpose, one of the approaches is correlation-based methods, *e.g.* the method based on Modal Assurance Criteria (MAC) Kim and Kim (2000). However, the MAC shows shortcomings in some situations. In the next section, these problems are elaborated and an alternative method to solve the issues is proposed.

4.1.1 Dealing with spatial aliasing

Historically, the MAC was developed to measure the consistency between different estimates of a modal vector Allemang (2003). It works properly for systems with well-separated resonance frequencies and with many response locations for the representation of modal vectors. However, when few sensors are available to estimate the experimental modal vectors, high MAC correlations may occur between modal vectors of the modes associated with different resonance frequencies. This is the spatial aliasing phenomenon which is related to observability of the system. Observability indicates the ability of the system to determine the internal states by the knowledge of the selected system outputs. An LTI system, with $\boldsymbol{A} \in \mathbb{C}^{2N \times 2N}$ is said to be observable if its observability matrix $\mathcal{O}(\boldsymbol{A}, \boldsymbol{C})$ has full rank, *i.e.*

$$rank(\mathcal{O}(\boldsymbol{A}, \boldsymbol{C})) = rank \begin{bmatrix} \boldsymbol{C} \\ \boldsymbol{CA} \\ \vdots \\ \boldsymbol{CA}^{2N-1} \end{bmatrix} = 2N \tag{18}$$

The relationship between the system's observability and modal properties is thus of special interest and motivated the development of the Modal Observability Correlation (MOC) metric, first proposed in Yaghoubi and Abrahamsson (2014). To this end, let $\mathcal{O}(\bar{\boldsymbol{A}}, \bar{\boldsymbol{C}})$ be the observability matrix of a linear system presented in the modal form,

$$\mathcal{O}(\bar{\boldsymbol{A}}, \bar{\boldsymbol{C}}) = \begin{bmatrix} \boldsymbol{C\Phi} \\ \boldsymbol{C\Phi\Lambda} \\ \vdots \\ \boldsymbol{C\Phi\Lambda}^{2N-1} \end{bmatrix} = \begin{bmatrix} \boldsymbol{C\phi}_1 & \boldsymbol{C\phi}_2 & \dots & \boldsymbol{C\phi}_{2N} \\ \boldsymbol{C\phi}_1\boldsymbol{\lambda}_1 & \boldsymbol{C\phi}_2\boldsymbol{\lambda}_2 & \dots & \boldsymbol{C\phi}_{2N}\boldsymbol{\lambda}_{2N} \\ \vdots & \vdots & \ddots & \vdots \\ \boldsymbol{C\phi}_1\boldsymbol{\lambda}_1^{2N-1} & \boldsymbol{C\phi}_2\boldsymbol{\lambda}_2^{2N-1} & \dots & \boldsymbol{C\phi}_{2N}\boldsymbol{\lambda}_{2N}^{2N-1} \end{bmatrix} \tag{19}$$

then, the modal observability vectors, $\wr_i, i = 1, 2, \dots, 2N$, are defined as the columns of the modal observability matrix, *i.e.*

$$\mathcal{O}(\boldsymbol{x}) = \mathcal{O}(\bar{\boldsymbol{A}}(\boldsymbol{x}), \bar{\boldsymbol{C}}(\boldsymbol{x})) = \begin{bmatrix} \wr_1(\boldsymbol{x}) & \wr_2(\boldsymbol{x}) & \dots & \wr_{2N}(\boldsymbol{x}) \end{bmatrix} \tag{20}$$

Each modal observability vector has the following important properties: (i) it contains information related to only one single vibrational mode, (ii) it includes the information of both eigenvector and eigenvalue, (iii) it relates the modal parameters to the observability of the modes given by a used sensor configuration. These properties suggest replacing eigenvectors in MAC by the modal observability vectors. Hence, for the correlation between two modal observability matrices $\mathcal{O}(\boldsymbol{x}_i)$ and $\mathcal{O}(\boldsymbol{x}_j)$, we have

$$\mathrm{MOC}(\mathcal{O}(\boldsymbol{x}_i), \mathcal{O}(\boldsymbol{x}_j)) = \frac{|\mathcal{O}(\boldsymbol{x}_i)^* \mathcal{O}(\boldsymbol{x}_j)|^2}{|\mathcal{O}(\boldsymbol{x}_i)^* \mathcal{O}(\boldsymbol{x}_i)||\mathcal{O}(\boldsymbol{x}_j)^* \mathcal{O}(\boldsymbol{x}_j)|}, \tag{21}$$

We call this metric the Modal Observability Correlation (MOC)[2]. Due to the property (ii) of the vectors $\wr_i, \quad i = 1, 2, \dots, 2N$, this metric discriminates between two highly correlated modal vectors with non-coinciding eigenvalues. This thus, makes MOC more powerful than MAC in dealing with the problem of spatial aliasing. It should be mentioned that raising the exponent of $\boldsymbol{\Lambda}$, see Eq.(19), may cause numerical problems. In order to avoid that, the MOC is evaluated for the eigenvalues of the discrete-time system which are located in the complex plane unit disc. This means, the eigenvalues of the continuous-time systems, $\lambda_j, j = 1, 2, \dots, 2N$ are transformed to the discrete-time counterpart using $\lambda_j^{\mathrm{disc}} = \exp(\lambda_j \tau)$ with an arbitrary time step τ. Here, $\tau = \pi / f_{max}$ in which f_{max} is the maximum eigenfrequency of the system. This leads to a distribution of the discrete-time eigenvalues $\lambda_j^{\mathrm{disc}}$ over a large domain of the unit disc and thus separates them well.

4.1.2 Dealing with coalescent eigenvalues

Due to the nonunique eigenvectors of coalescent or closely spaced eigenvalues, their presence in one system become one of the major challenges in both mode tracking and modal domi-

[2]This is called bMOC in Yaghoubi and Abrahamsson (2014)

nancy analysis. Therefore, it should be handled before any correlation analysis or dominancy analysis takes place.

For this purpose, let $\boldsymbol{\Phi}_j \in \mathbb{C}^{2N\times n_c}$ represent a matrix containing the linear independent eigenvectors associated with a coalescent eigenvalue λ_j of multiplicity n_c[3]. Moreover, let $\boldsymbol{V}$ be the n_c-dimensional space spanned by the columns of $\boldsymbol{\Phi}_j$. Since this is an A-invariant subspace of $\mathbb{C}^{2N}$, any vector that lies there can be considered as an eigenvector corresponding to λ_j. Therefore, different variants of a linearly independent basis for $\boldsymbol{V}$ may appear in repeated system realizations. To treat this issue, a fixed orthogonal basis for $\boldsymbol{V}$ is established by applying the QR-decomposition method on the projection of the columns of the system input matrix $\boldsymbol{B}$ onto $\boldsymbol{V}$, *i.e.* $\mathcal{P}_{\boldsymbol{V}}(\boldsymbol{B})$. That is,

$$\mathcal{P}_{\boldsymbol{V}}(\boldsymbol{B}) = \boldsymbol{\Phi}_j(\boldsymbol{\Phi}_j^*\boldsymbol{\Phi}_j)^{-1}\boldsymbol{\Phi}_j^*\boldsymbol{B} \tag{22}$$

where $\mathcal{P}_{\boldsymbol{V}}(\boldsymbol{B}) \in \mathbb{C}^{2N\times n_u}$. The QR-decomposition of $\mathcal{P}_{\boldsymbol{V}}(\boldsymbol{B})$ gives

$$\mathcal{P}_{\boldsymbol{V}}(\boldsymbol{B}) = \boldsymbol{Q}\boldsymbol{R} \tag{23}$$

here, $\boldsymbol{Q} \in \mathbb{C}^{2N\times 2N}$ is an orthogonal matrix and $\boldsymbol{R} \in \mathbb{R}^{2N\times n_u}$ is an upper triangular matrix. The fixed orthogonal basis for $\boldsymbol{V}$ can then be constructed by the first n_c columns of $\boldsymbol{Q}$, *i.e.* ,

$$\boldsymbol{V} = \mathrm{Span}(q_1, q_2, \ldots, q_{n_c}) \tag{24}$$

The space spanned by the columns q_i is also A-invariant and thus the unique vectors $q_i, i = 1, 2, \ldots, n_c$ are eigenvectors associated with the coalescent eigenvalues, λ_j Laub (2005). By that, the problem of nonunique eigenvector of coalescent eigenvalues is circumvented. This decomposition will be employed throughout this study to fix the eigenvectors of coalescent modes which may appear in the realization stage.

4.2 Modal dominancy analysis based on modal contribution into system input/output relation

Given an SS model of a dynamical system $\boldsymbol{\Sigma}$, by performing Laplace transformation, its transfer function can be obtained as

$$\boldsymbol{G}(s) = \boldsymbol{C}(s\boldsymbol{I}_{2N} - \boldsymbol{A})^{-1}\boldsymbol{B} + \boldsymbol{D}, \quad s \in \mathbb{C} \tag{25}$$

Assume $\bar{\boldsymbol{\Sigma}} = \boldsymbol{\Phi}(\boldsymbol{\Sigma})$ as presented in Eq. (7) is its associated minimal modal realization, and let

$$G_{(-i)}(s) = \frac{\bar{c}_i\bar{b}_i}{s - \lambda_i} \tag{26}$$

[3]Due to the controllability reasons, the dimension n_c cannot exceed the number of actuators, n_u.

be the transfer function of the error system resulting from deflation of the i^{th} modal coordinate from $\bar{\boldsymbol{\Sigma}}$. Then, the contribution of the i^{th} modal coordinate to the input-output relation of the system in the $\mathscr{H}_2$ sense can be defined as Rahrovani et al. (2014),

$$MC_{\mathscr{H}_2} = \|G_{(-i)}(j\omega)\|_{\mathscr{H}_2} = \frac{1}{\pi}\mathrm{tr}\{\bar{b}_i^* \bar{c}_i^* \bar{c}_i \bar{b}_i\}[\frac{1}{\mathfrak{Re}(\lambda_i)}\arctan(\frac{\omega}{\mathfrak{Re}(\lambda_i)})]_{-|\mathfrak{Im}(\lambda_i)|}^{\infty} \tag{27}$$

Here $(\bullet)^*$ stands for Hermitian operation, $\mathfrak{Re}$ and $\mathfrak{Im}$ respectively, denote real and imaginary parts of a complex number. $\mathscr{H}_2$ norm indicates the average error over frequency range of interest induced by removing the i^{th} modal coordinate Antoulas (2005). In general, it can be assumed that the more important a mode is, the larger will be its contribution to the input-output relation. Therefore, this measure can be a useful indication of dominancy for the modes. By using it, a system can be partitioned into two subsystems: a dominant and a weak one. The dominant one can be thus chosen as the reduced model. Let the system $\bar{\boldsymbol{\Sigma}}$ in Eq. (7) be partitioned as,

$$\begin{aligned}
\begin{bmatrix}\dot{\bar{\boldsymbol{\eta}}}_1(t)\\ \dot{\bar{\boldsymbol{\eta}}}_2(t)\end{bmatrix} &= \begin{bmatrix}\bar{\boldsymbol{A}}_{11} & \bar{\boldsymbol{A}}_{12}\\ \bar{\boldsymbol{A}}_{21} & \bar{\boldsymbol{A}}_{22}\end{bmatrix}\begin{bmatrix}\bar{\boldsymbol{\eta}}_1(t)\\ \bar{\boldsymbol{\eta}}_2(t)\end{bmatrix} + \begin{bmatrix}\bar{\boldsymbol{B}}_1\\ \bar{\boldsymbol{B}}_2\end{bmatrix}\boldsymbol{u}(t)\\
\bar{\boldsymbol{y}}(t) &= \begin{bmatrix}\bar{\boldsymbol{C}}_1 & \bar{\boldsymbol{C}}_2\end{bmatrix}\begin{bmatrix}\bar{\boldsymbol{\eta}}_1(t)\\ \bar{\boldsymbol{\eta}}_2(t)\end{bmatrix} + \bar{\boldsymbol{D}}\boldsymbol{u}(t)
\end{aligned} \tag{28}$$

then, a reduced-order model can be obtained by truncating $\bar{\boldsymbol{\eta}}_2$,

$$\begin{aligned}
\dot{\bar{\boldsymbol{\eta}}}_1(t) &= \bar{\boldsymbol{A}}_{11}\bar{\boldsymbol{\eta}}_1(t) + \bar{\boldsymbol{B}}_1\boldsymbol{u}(t)\\
\bar{\boldsymbol{y}}(t) &= \bar{\boldsymbol{C}}_1\bar{\boldsymbol{\eta}}_1(t) + \bar{\boldsymbol{D}}\boldsymbol{u}(t)
\end{aligned} \tag{29}$$

or residualizing $\bar{\boldsymbol{\eta}}_2$, *i.e.* $\dot{\bar{\boldsymbol{\eta}}}_2 = 0$,

$$\begin{aligned}
\dot{\bar{\boldsymbol{\eta}}}_1(t) &= \bar{\boldsymbol{A}}_{11}\bar{\boldsymbol{\eta}}_1(t) + \bar{\boldsymbol{B}}_1\boldsymbol{u}(t)\\
\bar{\boldsymbol{y}}(t) &= \bar{\boldsymbol{C}}_1\bar{\boldsymbol{\eta}}_1(t) + (\bar{\boldsymbol{C}}_2\bar{\boldsymbol{A}}_{22}^{-1}\bar{\boldsymbol{B}}_2 + \bar{\boldsymbol{D}})\boldsymbol{u}(t)
\end{aligned} \tag{30}$$

Readers interested in detailed discussions about this method are referred to Antoulas (2005).

4.3 PCE-based reduced order model

As mentioned in Def. 1, one system can have numerous equivalent systems, therefore after realizations and before interpolation, one should transform the systems such that they all have the same orientation. Therefore, the proposed method is presented as a two-step method. Step I is to perform isometric transformations and step II is to calculate the corresponding polynomial chaos expansion.

4.3.1 Step I: Isometric transformation

In this section, a proper isometric transformation is presented. In order to keep the diagonal form of the models, transformations are applied to each individual state separately. For

this purpose, first, one system is chosen as the reference model $\bar{\boldsymbol{\Sigma}}^{ref}$ and the others are transformed such that their modes have the same order and orientation as the reference ones. These transformations, illustrated in Fig. 1 for a 2-DOF system, are:

1. Permutation transformation $\mathcal{P}$: This transformation is devised to track the modes and treat the mode crossing phenomenon which is frequently occurred when parameters are varying in a system. For this purpose, each system is compared to the reference by using MOC and then its associated observability columns are permuted to obtain a diagonal MOC matrix, *i.e.* for $j = 1, 2, .., N_{ED}$

$$\mathcal{P}(\bar{\boldsymbol{\Sigma}}^{(j)}) = \{\mathcal{P}^{(j)} | diag(\mathrm{MOC}(\mathcal{O}^{(j)}, \mathcal{O}^{ref})\mathcal{P}^{(j)}) = diag(\sqrt{}^{1}, \sqrt{}^{2}, \ldots, \sqrt{}^{2N})\}, \tag{31}$$

in which

$$\sqrt{}^{i} = \max(\mathrm{MOC}(\lambda_i^{(j)}, \mathcal{O}^{ref})), \quad i = 1, 2, \ldots, 2N \tag{32}$$

The transformed system is thus,

$$\hat{\boldsymbol{\Sigma}}^{(j)} = \mathcal{P}(\bar{\boldsymbol{\Sigma}}^{(j)}) = \mathcal{P}\{\bar{\boldsymbol{A}}, \bar{\boldsymbol{B}}, \bar{\boldsymbol{C}}, \boldsymbol{D}\} = \{\hat{\boldsymbol{A}}, \hat{\boldsymbol{B}}, \hat{\boldsymbol{C}}, \boldsymbol{D}\} \tag{33}$$

Fig. 1a and Fig. 1b, respectively, illustrate eigenvectors of a 2-DOF system as are realized and after applying the permutation $\mathcal{P}$. The influence of this transformation can be simply observed.

2. Rotation transformation $\mathcal{R}$: This transformation could be obtained by minimizing the distance between the $\hat{\boldsymbol{c}}_i$ and $\bar{\boldsymbol{c}}_i^{ref}$ in a suitable norm. This can translate as the following minimization problem,

$$\min_{\nabla_i \in \mathbb{C}} \|\hat{\boldsymbol{c}}_i \nabla_i - \bar{\boldsymbol{c}}_i^{ref}\|_F^2, \quad i = 1, 2, \ldots, 2N \tag{34}$$

in which $\|\bullet\|_F$ stands for the Frobenius norm. The solution to this minimization problem is simply the projection of $\hat{\boldsymbol{c}}_i$ into the direction of $\bar{\boldsymbol{c}}_i^{ref}$, *i.e.* for $i = 1, 2, \ldots, 2N$

$$\nabla_i = \frac{\hat{\boldsymbol{c}}_i^{\mathsf{T}} \bar{\boldsymbol{c}}_i^{ref}}{\|\hat{\boldsymbol{c}}_i^{\mathsf{T}} \bar{\boldsymbol{c}}_i^{ref}\|}, \tag{35}$$

and therefore, the associated state is transformed as

$$\{\tilde{\lambda}_i, \tilde{\boldsymbol{b}}_i, \tilde{\boldsymbol{c}}_i\} = \nabla_i(\{\hat{\lambda}_i, \hat{\boldsymbol{b}}_i, \hat{\boldsymbol{c}}_i\}) = \{\nabla_i^{-1}\hat{\lambda}_i\nabla_i, \nabla_i^{-1}\hat{\boldsymbol{b}}_i, \hat{\boldsymbol{c}}_i\nabla_i\}, \tag{36}$$

and the rotated system can be thus written as

$$\tilde{\boldsymbol{\Sigma}}^{(j)} = \mathcal{R}(\hat{\boldsymbol{\Sigma}}^{(j)}) = \mathcal{R}\{\hat{\boldsymbol{A}}, \hat{\boldsymbol{B}}, \hat{\boldsymbol{C}}, \boldsymbol{D}\} = \{\tilde{\boldsymbol{A}}, \tilde{\boldsymbol{B}}, \tilde{\boldsymbol{C}}, \boldsymbol{D}\}, \quad j = 1, 2, .., N_{ED} \tag{37}$$

here $\mathcal{R} = diag(\nabla_1, \nabla_2, \ldots, \nabla_{2N})$, $\tilde{\boldsymbol{A}} = diag(\tilde{\lambda}_1, \tilde{\lambda}_2, \ldots, \tilde{\lambda}_{2N})$, $\tilde{\boldsymbol{B}} = [\tilde{\boldsymbol{b}}_1, \tilde{\boldsymbol{b}}_2, \ldots, \tilde{\boldsymbol{b}}_{2N}]$ and $\tilde{\boldsymbol{C}} = [\tilde{\boldsymbol{c}}_1, \tilde{\boldsymbol{c}}_2, \ldots, \tilde{\boldsymbol{c}}_{2N}]$. Fig. 1c shows the effect of the transformation $\mathcal{R}$ on the direction of the eigenvectors.

As can be observed, applying these two transformations to each individual realized system resulted in the systems as similar to the reference system as possible and they are thus ready for interpolation.

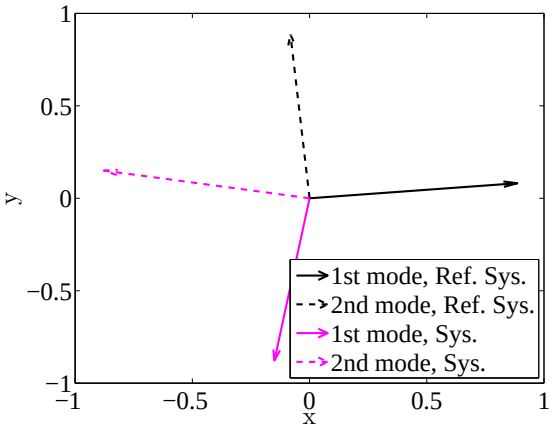

(a) Realized system

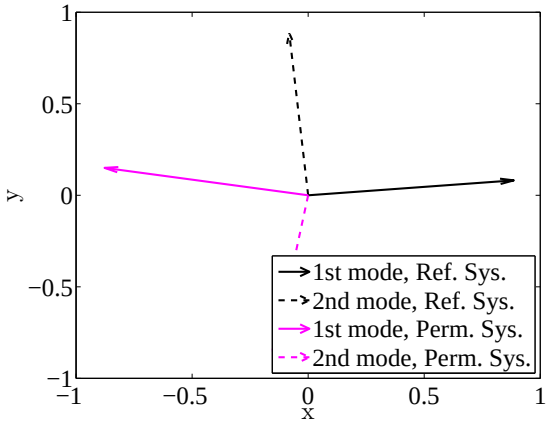

(b) After permutation $\mathcal{P}$

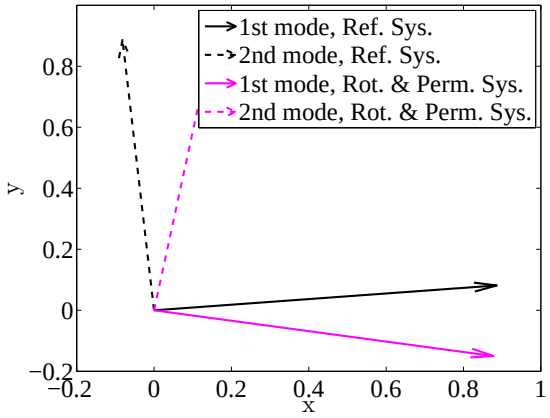

(c) After rotation $\mathcal{R}$

Figure 1: Illustration of isometric transformations for a 2-DOF system

4.3.2 Step II: Regression by PCE

The proposed approach is based on model reduction by utilizing the modal dominancy analysis. That is, the modal contribution as the mean of the modal dominancy is one of the important system properties which should be accurately predicted by the use of PCE. Therefore, two sets of PCE are requried: one for the modal contributions and one for the system matrices.

After applying the transformations to the systems, all the systems have the same mode order and mode orientations and thus, are ready to make PCE. For this purpose, systems matrices are collected in $\boldsymbol{\mathcal{S}}$ and their associated modal contributions are grouped in $\boldsymbol{\mathcal{MC}}_{\mathscr{H}_2}$ as follows,

$$\boldsymbol{\mathcal{S}} = \{\tilde{\boldsymbol{\Sigma}}^{(1)}, \tilde{\boldsymbol{\Sigma}}^{(2)}, \ldots, \tilde{\boldsymbol{\Sigma}}^{(N_{ED})}\} = \begin{bmatrix} \{diag(\tilde{\boldsymbol{A}}^{(1)}), vect(\tilde{\boldsymbol{B}}^{(1)}), vect(\tilde{\boldsymbol{C}}^{(1)}), vect(\boldsymbol{D}^{(1)})\}) \\ \{diag(\tilde{\boldsymbol{A}}^{(2)}), vect(\tilde{\boldsymbol{B}}^{(2)}), vect(\tilde{\boldsymbol{C}}^{(2)}), vect(\boldsymbol{D}^{(2)})\} \\ \vdots \\ \{diag(\tilde{\boldsymbol{A}}^{(N_{ED})}), vect(\tilde{\boldsymbol{B}}^{(N_{ED})}), vect(\tilde{\boldsymbol{C}}^{(N_{ED})}), vect(\boldsymbol{D}^{(N_{ED})})\} \end{bmatrix} \tag{38}$$

$$\boldsymbol{\mathcal{MC}}_{\mathscr{H}_2} = [\mathcal{MC}_{1,\mathscr{H}_2}, \mathcal{MC}_{2,\mathscr{H}_2}, \ldots, \mathcal{MC}_{N,\mathscr{H}_2}] \tag{39}$$

in which $diag(\cdot)$ stands for diagonal elements of the matrix $(\cdot)$, $vect(\cdot)$ denotes vectorizing operation,

$$\mathcal{MC}_{i,\mathscr{H}_2} = [MC^{(1)}_{i,\mathscr{H}_2}, MC^{(2)}_{i,\mathscr{H}_2}, \ldots, MC^{(N_{ED})}_{i,\mathscr{H}_2}]^T \quad i = 1, 2, \ldots, N,$$

here $(\cdot)^T$ denotes transpose operation.

In order to make PCE, since system's matrices are normally complex-valued whereas, the PCE which is selected as the regression method here, is only defined for real-valued functions[4], separate PCEs need to be performed for real and imaginary parts of the $\boldsymbol{\mathcal{S}}$. Note that, PCE could also be made for amplitude and phase of the $\boldsymbol{\mathcal{S}}$ however, based on the authors' experience, expansions on real and imaginary parts are more robust. Therefore, the matrices $\boldsymbol{\mathcal{S}}^{\mathfrak{Re}} = real(\boldsymbol{\mathcal{S}})$ and $\boldsymbol{\mathcal{S}}^{\mathfrak{Im}} = imag(\boldsymbol{\mathcal{S}})$ are the matrices for which the PCE should be made. Besides that, a system's matrices normally occur in complex conjugate pairs. It means that PCE can be made only for one of each pair and the other will be constructed afterward, *i.e.* $\boldsymbol{\mathcal{S}} \in \mathbb{C}^{N_{ED} \times (N(1+n_u+n_y)+n_u \times n_y)}$.

The number of random outputs for this set, $N_Y = 2 \times N_{ED} \times (N(1+n_u+n_y)+n_u \times n_y)$, can be extremely large. As discussed in Section 3.2, the PCEs are therefore applied directly to the principal components of $\boldsymbol{\mathcal{S}}$, yielding:

$$\hat{\boldsymbol{\mathcal{S}}}^{\mathfrak{Re}} = \mathbb{E}\left[\boldsymbol{\mathcal{S}}^{\mathfrak{Re}}\right] + \sum_{j=1}^{\hat{N}_Y} \sum_{\boldsymbol{\alpha} \in \mathcal{A}^{M,p}} (u^{\mathfrak{Re}}_{\boldsymbol{\alpha}} \psi_{\boldsymbol{\alpha}}(\boldsymbol{x}))_j \boldsymbol{v}_j^{\mathfrak{Re}^{\mathrm{T}}}, \tag{40}$$

$$\hat{\boldsymbol{\mathcal{S}}}^{\mathfrak{Im}} = \mathbb{E}\left[\boldsymbol{\mathcal{S}}^{\mathfrak{Im}}\right] + \sum_{j=1}^{\hat{N}_Y} \sum_{\boldsymbol{\alpha} \in \mathcal{A}^{M,p}} (u^{\mathfrak{Im}}_{\boldsymbol{\alpha}} \psi_{\boldsymbol{\alpha}}(\boldsymbol{x}))_j \boldsymbol{v}_j^{\mathfrak{Im}^{\mathrm{T}}}, \tag{41}$$

where $u^{\mathfrak{Re}}_{\boldsymbol{\alpha}}$ and $u^{\mathfrak{Im}}_{\boldsymbol{\alpha}}$ are respectively the vectors of coefficients of the PCEs made for the real and imaginary parts of the $\tilde{\boldsymbol{\mathcal{S}}}$.

The next set of PCE will be made for the modal contributions collected in the matrix $\boldsymbol{\mathcal{MC}}_{\mathscr{H}_2}$. Since the number of random outputs for this set is not very large, PCE can be applied directly to them *i.e.* for $i = 1, 2, \cdots, N$

$$\hat{\mathcal{MC}}_{i,\mathscr{H}_2} = \sum_{\boldsymbol{\alpha} \in \mathcal{A}^{M,p}} mc^{\mathscr{H}_2}_{\boldsymbol{\alpha}}(i) \psi_{\boldsymbol{\alpha}}(\boldsymbol{x}). \tag{42}$$

[4]Limited literature is available on the use of PCE for complex-valued functions, see *e.g.* Soize and Ghanem (2004).

where $mc^{\mathscr{H}_2}$ is the vector of coefficients of the PCEs. The proposed approach is formulated in Algorithm 1.

4.3.3 PCE-based model reduction and response prediction

In order to obtain a reduced model at new sample point $\boldsymbol{x}^{(0)}$, one can evaluate the whole PCE-based SS model to make a full-order system and then reduce it using any truncation scheme, or alternatively, select the dominant modes and evaluate PCEs only at those modes to make a reduced-order SS model. Latter has been selected in this paper due to its efficiency in time and memory usage.

For this purpose, two steps should be taken: (i) PCE-based model reduction, and (ii) PCE-based model prediction. For the first step, one should evaluate Eq. (42) to obtain contribution of the modes $\hat{\mathcal{MC}}_{i,\mathscr{H}_2} \quad i = 1, 2, \cdots, N$ and then, sort them in right order to determine the first n modes to construct the dominant subsystem, see Eq. (28).

As the second step, Eqs. (40) and (41) are evaluated for the n selected modes to obtain $\hat{\boldsymbol{\mathcal{S}}}_r^{\mathfrak{Re}}(\boldsymbol{x}^{(0)})$ and $\hat{\boldsymbol{\mathcal{S}}}_r^{\mathfrak{Im}}(\boldsymbol{x}^{(0)})$, respectively. Then the matrix $\hat{\boldsymbol{\mathcal{S}}}_r(\boldsymbol{x}^{(0)}) \in \mathbb{C}^{1\times(n(1+n_u+n_y)+n_u\times n_y)}$ can be constructed by $\hat{\boldsymbol{\mathcal{S}}}_r^{\mathfrak{Re}}(\boldsymbol{x}^{(0)}) + j\hat{\boldsymbol{\mathcal{S}}}_r^{\mathfrak{Im}}(\boldsymbol{x}^{(0)}), \quad j = \sqrt{-1}$ and in turn, the system matrices can be constructed by an inverse vectorization operation. The algorithm for predicting the response of the reduced model at a new sample point is briefly presented in Algorithm 2.

Algorithm 1 Proposed PCE-based surrogate modeling for SS models

Input: $\boldsymbol{\mathcal{X}} = \{\boldsymbol{x}^{(1)}, \boldsymbol{x}^{(2)}, ..., \boldsymbol{x}^{(N_{ED})}\}$

Step I: Isometric transformations

$\bar{\boldsymbol{\Sigma}}^{ref}$=$\{\bar{\boldsymbol{\Sigma}}(\boldsymbol{x}^{(r)})\}$=$\{\bar{\boldsymbol{A}}(\boldsymbol{x}^{(r)}), \bar{\boldsymbol{B}}(\boldsymbol{x}^{(r)}), \bar{\boldsymbol{C}}(\boldsymbol{x}^{(r)}), \boldsymbol{D}(\boldsymbol{x}^{(r)})\}$, for a random $r \in [1, ..., N_{ED}]$

for $k = 1$ **to** N_{ED} **do**

  $\bar{\boldsymbol{\Sigma}}^{k}$=$\{\bar{\boldsymbol{\Sigma}}(\boldsymbol{x}^{(k)})\}$=$\{\bar{\boldsymbol{A}}(\boldsymbol{x}^{(k)}), \bar{\boldsymbol{B}}(\boldsymbol{x}^{(k)}), \bar{\boldsymbol{C}}(\boldsymbol{x}^{(k)}), \boldsymbol{D}(\boldsymbol{x}^{(k)})\}$ using Eq. (7)

  Compute permutation transformation $\mathcal{P}$ using Eq.(31)

  Evaluate $\hat{\boldsymbol{\Sigma}}^{k} = \mathcal{P}(\bar{\boldsymbol{\Sigma}}^{k}) = \mathcal{P}\{\bar{\boldsymbol{A}}, \bar{\boldsymbol{B}}, \bar{\boldsymbol{C}}, \boldsymbol{D}\} = \{\hat{\boldsymbol{A}}, \hat{\boldsymbol{B}}, \hat{\boldsymbol{C}}, \boldsymbol{D}\}$

  for $i = 1$ **to** N **do**

    Compute $\nabla_i = \frac{\hat{\boldsymbol{c}}_i^{\mathsf{T}} \bar{\boldsymbol{c}}_i^{ref}}{\|\hat{\boldsymbol{c}}_i^{\mathsf{T}} \bar{\boldsymbol{c}}_i^{ref}\|}$

  end for

  $\mathcal{R} = diag(\nabla_1, \nabla_2, \ldots, \nabla_N)$

  Evaluate $\tilde{\boldsymbol{\Sigma}}^{(k)} = \mathcal{R}(\hat{\boldsymbol{\Sigma}}^{(k)}) = \mathcal{R}\{\hat{\boldsymbol{A}}, \hat{\boldsymbol{B}}, \hat{\boldsymbol{C}}, \boldsymbol{D}\} = \{\tilde{\boldsymbol{A}}, \tilde{\boldsymbol{B}}, \tilde{\boldsymbol{C}}, \boldsymbol{D}\}$

  Evaluate $\boldsymbol{MC}_{\mathscr{H}_2}^{(k)} = [MC_{1,\mathscr{H}_2}^{(k)}, MC_{2,\mathscr{H}_2}^{(k)}, \ldots, MC_{N,\mathscr{H}_2}^{(k)}]$ using Eq. (27)

end for

Step II: Interpolation by PCE

$\boldsymbol{\mathcal{S}} = \{\tilde{\boldsymbol{\Sigma}}^{(1)}, \tilde{\boldsymbol{\Sigma}}^{(2)}, \ldots, \tilde{\boldsymbol{\Sigma}}^{(N_{ED})}\} \in \mathbb{C}^{N_{ED} \times (N(1+n_u+n_y)+n_u \times n_y)}$,

$\boldsymbol{\mathcal{S}}^{\mathfrak{Re}}$=real($\boldsymbol{\mathcal{S}}$), $\boldsymbol{\mathcal{S}}^{\mathfrak{Im}}$=imag($\boldsymbol{\mathcal{S}}$)

$\mathcal{MC}_{i,\mathscr{H}_2} = [MC_{i,\mathscr{H}_2}^{(1)}, MC_{i,\mathscr{H}_2}^{(2)}, \ldots, MC_{i,\mathscr{H}_2}^{(N_{ED})}]^T \quad i = 1, 2, \ldots, N,$

Polynomial chaos expansion,

$\hat{\boldsymbol{\mathcal{S}}}^{\mathfrak{Re}}$: PCE of $\boldsymbol{\mathcal{S}}^{\mathfrak{Re}}$ using Eq. (40)

$\hat{\boldsymbol{\mathcal{S}}}^{\mathfrak{Im}}$: PCE of $\boldsymbol{\mathcal{S}}^{\mathfrak{Im}}$ using Eq. (41)

$\hat{\mathcal{MC}}_{i,\mathscr{H}_2}$: PCE of $\mathcal{MC}_{i,\mathscr{H}_2}$ using Eq. (42), $\quad i = 1, 2, \ldots, N$

$\hat{\boldsymbol{\mathcal{MC}}}_{\mathscr{H}_2} = [\hat{\mathcal{MC}}_{1,\mathscr{H}_2}, \hat{\mathcal{MC}}_{2,\mathscr{H}_2}, \ldots, \hat{\mathcal{MC}}_{N,\mathscr{H}_2}]$

Output: $\hat{\boldsymbol{\mathcal{S}}}^{\mathfrak{Re}}$, $\hat{\boldsymbol{\mathcal{S}}}^{\mathfrak{Im}}$, $\hat{\boldsymbol{\mathcal{MC}}}_{\mathscr{H}_2}$

Algorithm 2 Predicting reduced system's responses

Input: $\boldsymbol{x}^{(0)} \neq \boldsymbol{x}^{(l)}, \quad l = 1, 2, ..., N_{ED}$

Step I: Model reduction:

---

for $i = 1$ **to** N **do**

  Evaluate $\hat{\mathcal{MC}}_{i,\mathscr{H}_2}(\boldsymbol{x}^{(0)})$ using Eq. (42)

end for

$\hat{\boldsymbol{\mathcal{MC}}}_{\mathscr{H}_2} = [\hat{\mathcal{MC}}_{1,\mathscr{H}_2}, \hat{\mathcal{MC}}_{2,\mathscr{H}_2}, \ldots, \hat{\mathcal{MC}}_{N,\mathscr{H}_2}]$

Sort $\hat{\boldsymbol{\mathcal{MC}}}_{\mathscr{H}_2}$ in right order and select first n dominant modes

Step II: Model construction:

Evaluate $\hat{\boldsymbol{\mathcal{S}}}_r^{\mathfrak{Re}} = \hat{\boldsymbol{\mathcal{S}}}^{\mathfrak{Re}}(\boldsymbol{x}^{(0)})$ using Eq. (40) for the n selected modes.

Evaluate $\hat{\boldsymbol{\mathcal{S}}}_r^{\mathfrak{Im}} = \hat{\boldsymbol{\mathcal{S}}}^{\mathfrak{Im}}(\boldsymbol{x}^{(0)})$ using Eq. (41) for the n selected modes.

$\hat{\boldsymbol{\mathcal{S}}}_r = \hat{\boldsymbol{\mathcal{S}}}_r^{\mathfrak{Re}} + j\hat{\boldsymbol{\mathcal{S}}}_r^{\mathfrak{Im}} \in \mathbb{C}^{1\times(n(1+n_u+n_y)+n_u\times n_y)}, \quad j = \sqrt{-1}$

Construct $\hat{\hat{\boldsymbol{\Sigma}}}_r^{(0)}$ from $\hat{\boldsymbol{\mathcal{S}}}_r$ by inverse vectorization and diagonalization operations

Output: $\hat{\hat{\boldsymbol{\Sigma}}}_r^{(0)} = \hat{\hat{\boldsymbol{\Sigma}}}_r(\boldsymbol{x}^{(0)})$

5 Case studies

5.1 Introduction

In this section, the proposed method will be applied to four case studies, (*i*) a simple 4-DOF system to illustrate how the method works, (*ii*) a 2-DOF system representing the complex phenomenon of mode veering, (*iii*) a 6-DOF system with a relatively large (16-dimensional) parameter space. (*iv*) a 3D Timoshenko cantilever beam representing a large-scale model. For the sake of readability, for the last two cases with 6 outputs, only results for one of the outputs are shown.

To assess the accuracy of the proposed PCE-based model reduction approach quantitatively, the following measure based on the root mean square (rms) error of the vectors is defined.

$$Error(\cdot) = \frac{\text{rms}((\cdot)^{ex} - (\cdot)^{approx}))}{\text{rms}((\cdot)^{ex})} \times 100\%, \tag{43}$$

in which $(\cdot)$ is a vector of interest which could be the frequency response of a system in a specific frequency band. $(\cdot)^{ex}$ and $(\cdot)^{approx}$ represent results obtained by the exact and the approximate model, respectively. The definition of exact and approximate model will be mentioned in the context.

Before analyzing the examples, following models should be described: (*i*) Full model: the true model with the order of $2N$, (*ii*) Direct reduced order model (ROM): the true model reduced to order of $2n$ by the method of dominancy analysis (*iii*) PCE-based ROM: the PCE-based model with the order of $2n$. It should be emphasized that, in all examples, the dominancy analysis has been carried out with state residualization technique, Eq. (30).

5.2 4-DOF system

As the first example, the simple 4-DOF system shown in Fig. 2 is selected to highlight the steps of the proposed method. This example is taken from Amsallem and Farhat Amsallem and Farhat (2011) and has been previously studied in Lohmann and Eid (2007). The system with one input at mass 4 and one output at mass 1 is shown in Fig. 2. It consists of 6 springs, 4 dampers and 4 masses which are specified as constant or as functions of a parameter μ in Table 1. The parameter μ is assumed to be uniformely distributed in $[0, 1]$. In this example the full model has the order of 8, *i.e.* $N = 4$, and the reduced models are chosen to have order 4, $n = 2$.

Since this system has one output, it can reveal the shortcoming of the MAC-based mode tracking in the cases with few number of sensors. The result of correlation analysis between the modes of a randomly selected system and the reference system is shown in Fig. 3. The numbers indicate the amount of correlation between the modes. They are between $[0, 1]$, ranging from no correlation to full correlation. The results show that MAC, Fig. 3a, cannot distinguish between the modes, whereas MOC can, Fig. 3b.

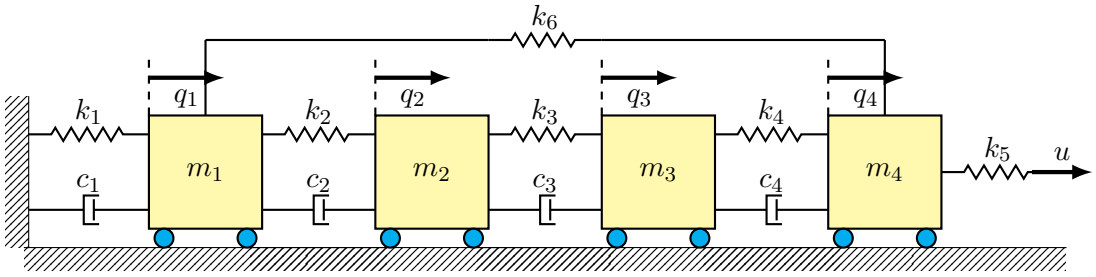

Figure 2: Simple 4-DOF system with parameters presented in Table 1

Table 1: The 4-DOF system's variables

Masses		Dampers		Stiffnesses	
	(Kg)		(Ns/m)		(N/m)
m_1	125	c_1	μ	k_1	$2+2\mu$
m_2	25	c_2	1.6	k_2	1
m_3	5	c_3	0.4	k_3	3
m_4	1	c_4	0.1	k_4	9
				k_5	27
				k_6	$1+2\mu$

Table 2: Error analysis based on Eq. (43) to construct a proper Experimental Design (ED)

# ED points	4	5	10
max(error) %	10.4	1.11	0.06

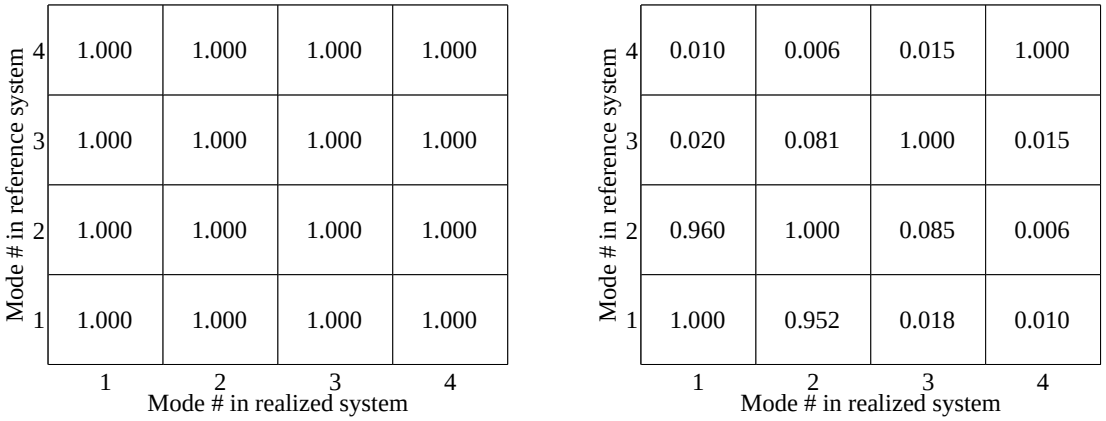

(a) MAC analysis

(b) MOC analysis

Figure 3: Correlation analysis between the modes of a realized system with the reference system.

In order to show the feasibility of the method and form a suitable Experimental Design (ED), maximum 1% error (Eq. (43)) between the PCE-based ROMs and Direct ROMs has been targeted. For this purpose, PCE-based ROMs were made by using different number of ED points and their accuracies have been assessed by comparing with their corresponding Direct ROMs over 10,000 Monte-Carlo samples extracted from the parameter space. The accuracy analysis was performed for each individual frequency response by using Eq. (43) in which $(\cdot)^{ex}$ was the Direct ROM and $(\cdot)^{approx}$ was the PCE-based ROM. The maximum error is reported in Table 2. It indicates that 5 points at $[0, 0.25, 0.5, 0.75, 1]$ are sufficient.

Their associated models and modal contributions are obtained to construct $\boldsymbol{\mathcal{S}}$ and $\boldsymbol{\mathcal{MC}}_{\mathscr{H}_2}$ to be prepared for making PCE.

The next step is to find a suitable basis and the associated coefficients for the polynomial chaos expansion. In this case, since the random variable μ is uniformly distributed, the basis of the polynomial chaos consists of Legendre polynomials. The LAR algorithm Blatman and Sudret (2011) is employed here to calculate a sparse PCE with adaptive degree. The efficient implementation of the LAR is available in the Matlab-based toolbox UQLab Marelli and Sudret (2014).

To validate the approach, 10,000 Monte-Carlo samples are extracted from the parameter space and both the true and PCE-based models are evaluated. Their accuracies are then assessed by comparing their associated properties as follows. Fig. 4a illustrates the contributions of each mode calculated from the true model and obtained by its associated PCE, Eq. (42). It indicates the PCE predicts the modal contributions accurately. Since reducing the model order will be carried out based on these contributions, this is a crucial result. Eigenvalues of the systems has been compared in Fig. 4b. High accuracy of the PCE-based model in prediting the eigenvalues can be simply observed.

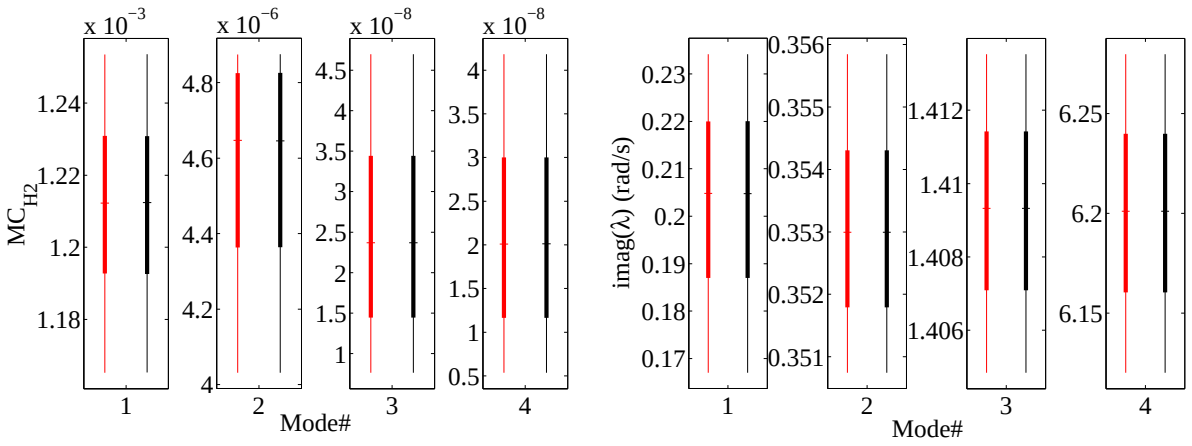

(a) Modal contributions

(b) Eigenfrequencies

Figure 4: System property comparison between the PCE-based model (in black) and the true model (in red) obtained over 10,000 points sampled from the parameter space

Frequency response functions (FRF) offer another means for assessing the overall accuracy of the PCE-based model by its comparison with that of the true model using Eq. (43). The FRF has been evaluated in the frequency band of $[0, 10]$ (rad/s). The error metric defined at Eq. (43) is used for comparison with the full model as $(\cdot)^{ex}$ and the reduced models as $(\cdot)^{approx}$. The results of this analysis, shown in Fig. 5, indicate that the maximum error, about 1.15%, occurs for $\mu = 0.154$. One can reduce this error by increasing the ED, as suggested by Table. 2. The model associated with this parameter value is thus

selected for detailed investigation, see Fig. 6. Comparison between the eigenvalues, Fig. 6a, and FRFs of the full model and the reduced models, Fig. 6b, reveal that the proposed method accurately predicts the reduced model. Moreover, Fig. 6c illustrates the error at each frequency defined in Eq. (43) when $(\cdot)^{ex}$ was the full true model and $(\cdot)^{approx}$ was the reduced models obtained by the modal dominancy analysis and the proposed PCE-based method. It indicates the accuracy of the proposed method. Large error at the end of the frequency range is due to the truncation of the last two modes. Moreover, the maximum difference between the Direct ROM and the PCE-based model, about 1%, has been occurred at the first resonant frequency. Since amplitudes at resonant frequencies are highly sensitive to the damping values, the main reason for this error could be the under(over) estimation of damping values obtained from the imaginary part of the eigenfrequencies collected in matrix $\boldsymbol{A}$. As mentioned, the accuracy could increase by increasing the ED size.

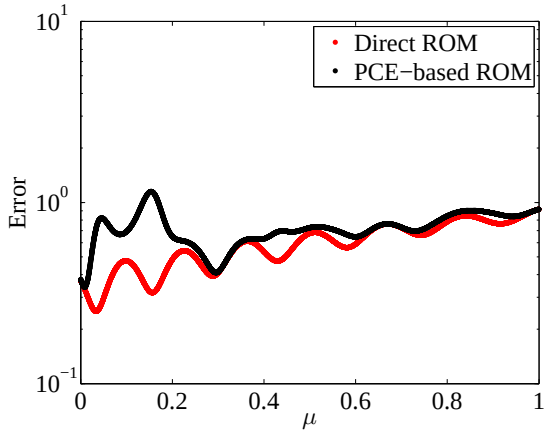

Figure 5: Error of the evaluated FRFs by changing the parameter μ

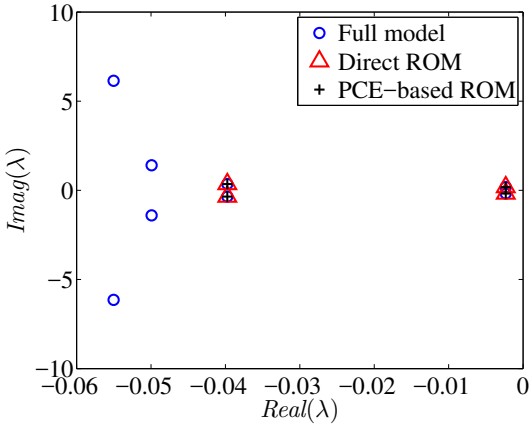

(a) Predicted eigenvalues

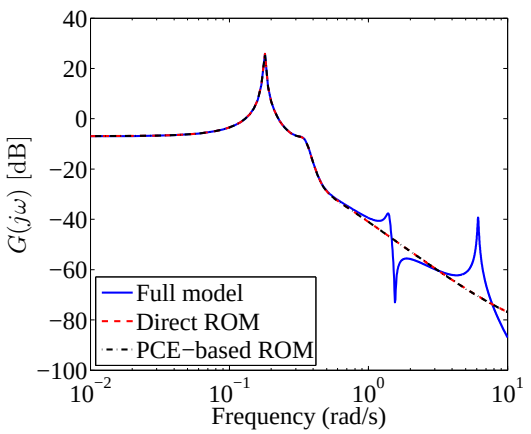

(b) Predicted FRF

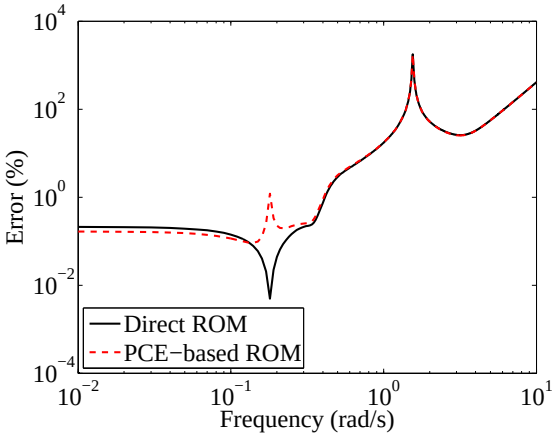

(c) Detailed error analysis

Figure 6: Detailed accuracy analysis for the least accurate predicted FRF among 10,000 Monte-Carlo samples which according to Fig. 5 occurs at $\mu = 0.154$

5.3 2-DOF system: mode veering

In this section, a 2-DOF system will be studied. This simple mechanical system, shown in Fig. 7, presents the complex mode veering phenomenon Morand and Ohayon (1995). This system is similar to the one studied in Amsallem and Farhat (2011); Stephen (2009). It is parameterized by the stiffness $k_1 = \mu$ which follows the lognormal distribution, $\mathcal{LN}(-0.02, 0.2)$, in which $\mathbb{E}[k_1] = 1$ and $\mathbb{E}[k_1^2] = 0.2$. The other properties of the system are listed in Table 3. Variation of the system's eigenvalues, shown in Fig. 8, together with changing the eigenvectors's directions indicate the mode veering phenomenon.

Fig. 1 illustrates the eigenvectors of the randomly selected system together with their associated reference ones. Fig. 1a shows the eigenvectors as they are realized for a value of μ. As expected, they are required to transform to be similar to their corresponding reference ones. Fig. 1b and 1c show the eigenvectors after permutation $\mathcal{P}$ and rotation $\mathcal{R}$, respectively.

As the first step of making PCE, a proper number of samples should be chosen for the

ED. For this purpose, prediction accuracy of the PCE-based model has been checked over the frequency range of [0.5, 1.8] rad/s on a large reference validation set. This set consists of 10,000 points sampled from the parameter space using the Monte-Carlo approach at which the response of the true model has been evaluated to estimate the reference mean and standard deviation. Then, the error (Eq.(43)) associated with the first two moments of the PCE-based models' responses made on experimental designs of increasing size are obtained by comparing with the corresponding reference results. The resulting convergence curves are given in Fig. 9. It implies that 300 points are necessary for the ED in this example, because for larger sizes the accuracy does not improve significantly.

Therefore, since this example presents a complex problem with large COV of the parameter, 300 sample points are extracted from the parameter space using the Sobol pseudorandom sampling Sobol (1990) and the associated models are obtained to design the experiment. To select the basis, note that $X \sim \mathcal{LN}(\lambda, \xi) \Leftrightarrow \ln(X) \sim \mathcal{N}(\lambda, \xi)$, thus, the Hermite polynomial is used as basis for $\ln(X)$.

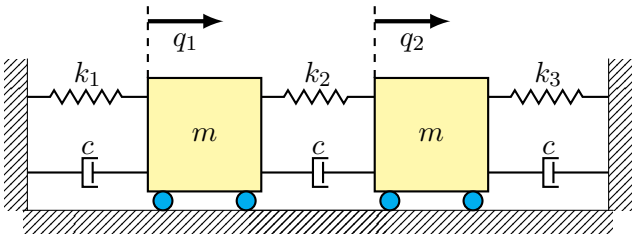

Figure 7: 2-DOF system presenting mode-veering phenomenon

Table 3: 2-DOF system's characteristic

Characteristics	$m[kg]$	$k_2[N/m]$	$k_3[N/m]$	$c[Ns/m]$
value	1	0.05	1	0.001

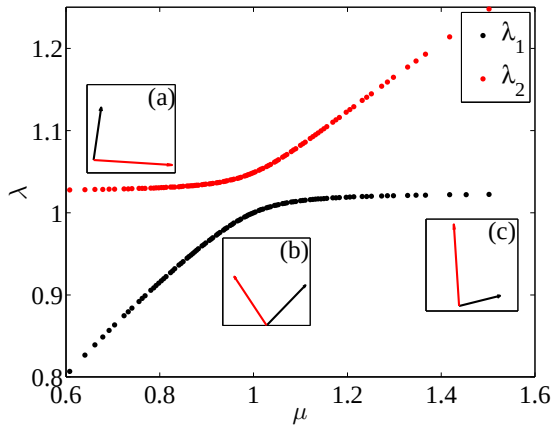

Figure 8: Mode veering phenomenon, (a) $\mu = 0.65$, (b) $\mu = 1$, (c) $\mu = 1.5$

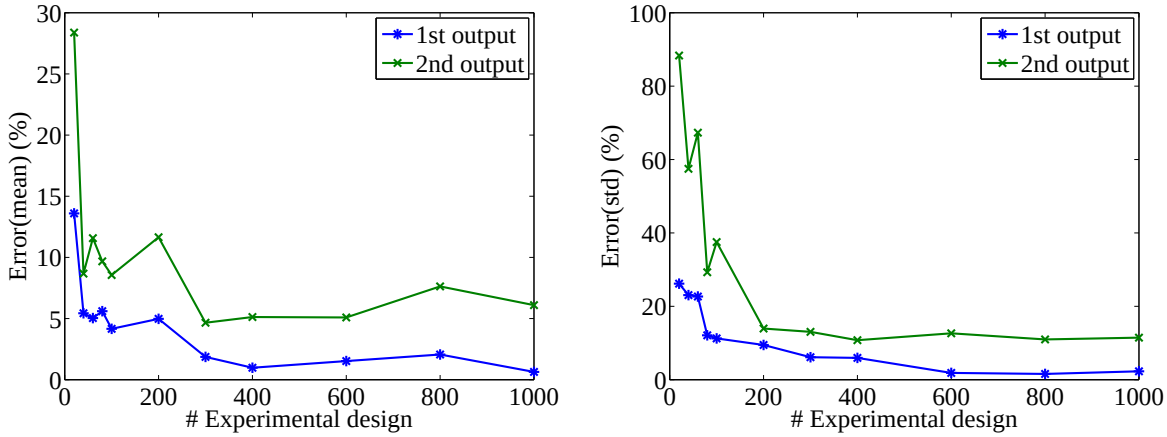

(a) Mean of the FRFs

(b) Standard deviation of the FRFS

Figure 9: Convergence analysis of the first two moments of the FRF to find a proper number of points for the experimental design.

The main objective of studying this example is to show the adequacy of the method in dealing with the complex case of mode veering phenomenon. Therefore, the 10,000 model evaluations used to produce the convergence curves in Fig. 9 are also used to provide a detailed validation of the performance of the PCE-based model. The results are presented as follows. Fig. 10a shows the eigenvalues of the true model on top of those of the PCE-based model. Their relative difference measured by

$$\frac{|\lambda_i^{ex} - \lambda_i^{approx}|}{|\lambda_i^{ex}|} \times 100\% \quad i = 1, 2$$

is shown in Fig. 10b. They indicate the competence of the method in predicting the variation of the eigenvalues when μ is varied. Moreover, using both the PCE-based model and the true model, FRFs are evaluated and compared using Eq. (43). The results of this accuracy analysis are shown in Fig. 11.

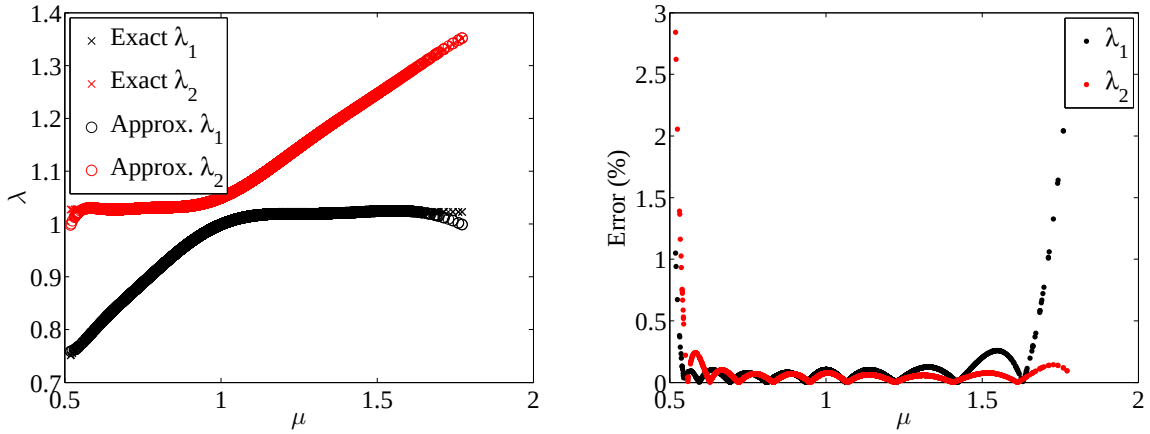

(a) Absolute values (b) Relative errors

Figure 10: Predicted eigenvalues evaluated by the true model and the PCE-based model

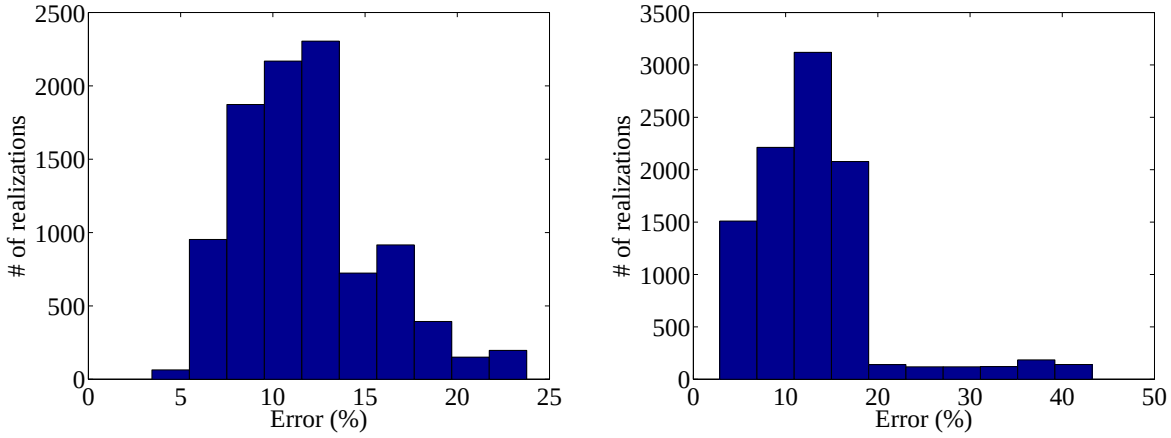

(a) 1st output (b) 2nd output

Figure 11: Accuracy analysis of the method by comparing the frequency response of the PCE-based model with that of the true model evaluated by Eq. (43).

In order to visualize the accuracy of method, two realizations were considered, namely one with a typical error, about 25% in total[5], and the one with the maximum error, about 65% in total[6]. They are presented in Figures 12 and 13, respectively. They indicate that even for the worst-case, the presented approach results in prediction of the system matrices and in turn, FRFs with excellent accuracy.

[5]Sum of average errors at the outputs, 12%+13%=25%

[6]Sum of maximum errors at the outputs, 22%+43%=65%

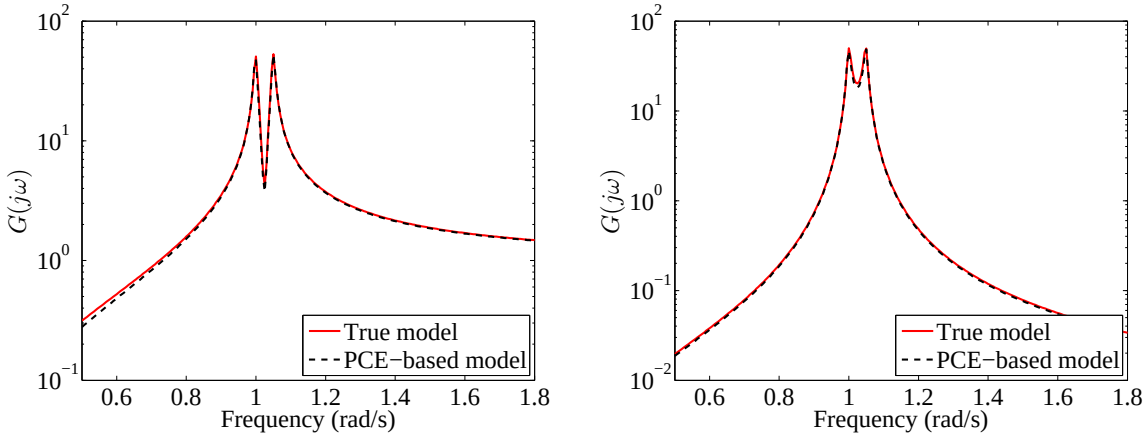

(a) First system output (b) Second system output

Figure 12: Typical FRF prediction, true (solid line) and predicted (dashed line) FRF of the system

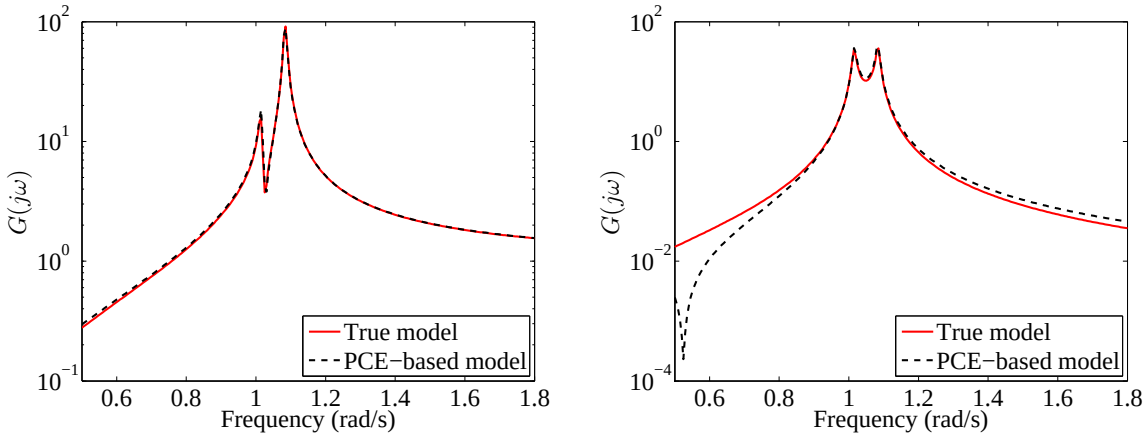

(a) First system output (b) Second system output

Figure 13: Worst case FRF prediction among 10,000 sample points, true (solid line) and predicted (dashed line) FRF of the system.

5.4 6-DOF system: large parameter space

The third example is chosen to illustrate the application of the proposed method to a problem with a relatively large parameter space. The system, shown in Fig. 14, has been studied before by Yaghoubi *et al.* in Yaghoubi et al. (2017). It consists of 10 springs and 6 masses which are modeled by random variables with lognormal distributions. Their mean values and Coefficient of Variations (COV) are listed in Table 4. The damping matrix is $\boldsymbol{V} = 0.01\widehat{\boldsymbol{M}}$, where $\widehat{\boldsymbol{M}}$ is the matrix of the mean value of the system masses.

The system with one input force at mass 6 and 6 system outputs, one for each mass, has order $2N = 12$ and we want to reduce it to $2n = 8$. In order to perform the accuracy

analysis, FRF of the system is evaluated at a frequency range from 0.1 to 4 Hz with the step of 0.01 Hz.

In this example, the ED consists of 1000 points sampled from the parameter space using Sobol sampling method. The marginal distributions of the input vectors $\boldsymbol{X}$ consists of lognormal distributions. Therefore, the chosen PCE basis consists of Hermite polynomials on the reduced variable $\boldsymbol{Z} = \ln(\boldsymbol{X})$. Eq. (10) thus, can be written as

$$\boldsymbol{Y} = \mathcal{M}(\boldsymbol{X}) = \sum_{\boldsymbol{\alpha} \in \mathcal{A}^{M,p}} \tilde{u}_{\boldsymbol{\alpha}} \, \psi_{\boldsymbol{\alpha}}(\ln(\boldsymbol{X})).$$

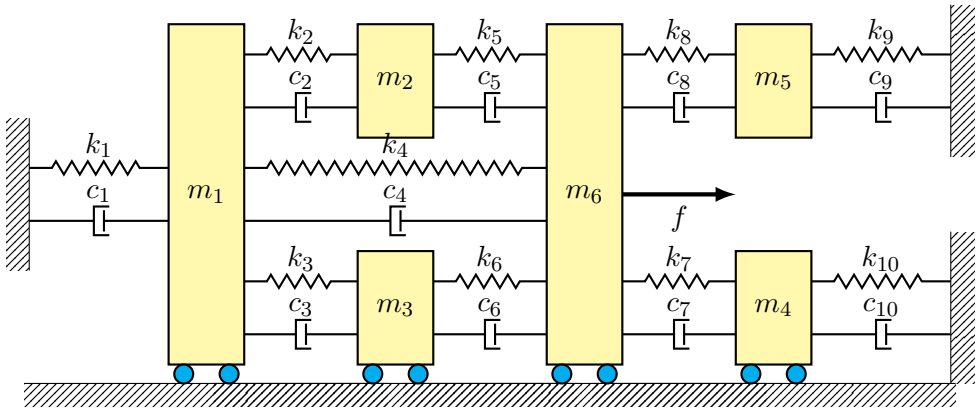

Figure 14: The 6-DOF system

Table 4: The 6-DOF system's variables

	Variables	mean	Coeff. of variation (%)
Masses $[kg]$	m_1	50	10
	m_2	35	10
	m_3	12	10
	m_4	33	10
	m_5	100	10
	m_6	45	10
Stiffnesses $[N/m]$	k_1	3000	10
	k_2	1725	10
	k_3	1200	10
	k_4	2200	10
	k_5	1320	10
	k_6	1330	10
	k_7	1500	10
	k_8	2625	10
	k_9	1800	10
	k_{10}	850	10

The LAR algorithm has been employed to build sparse PCEs with adaptive degree. Since the dimension of the input parameter space is large, to reduce the unknown coefficients of the PCEs and avoid the curse of dimensionality, a hyperbolic truncation with q-norm of 0.7 was used before the LAR algorithm. Besides, only polynomials up to rank 2 were selected here (*i.e.* polynomials that depend at most on 2 of the 16 parameters). It should be mentioned that all the PCEs used for the surrogate model have eventually maximum degrees less than 10.

In order to assess the accuracy of the PCE-based model in estimating various quantities of interests, 10,000 points sampled from the parameter space by using Monte-Carlo sampling at which both the true and the PCE-based models are evaluated and their associated properties have been compared in Fig. 15. Fig. 15a illustrates the contributions of each mode calculated from the true model and obtained by its associated PCE, Eq. (42). Eigenvalues of the systems have been compared in Fig. 15b.

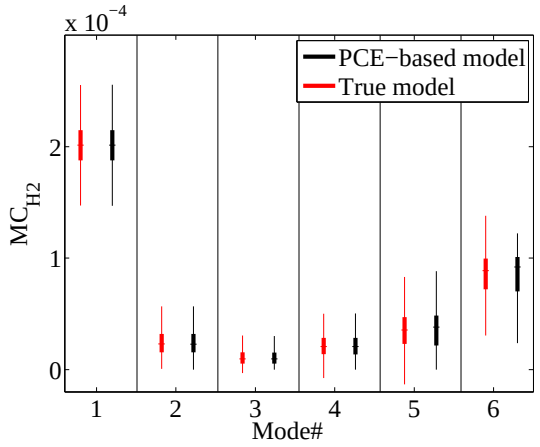

(a) Modal contributions

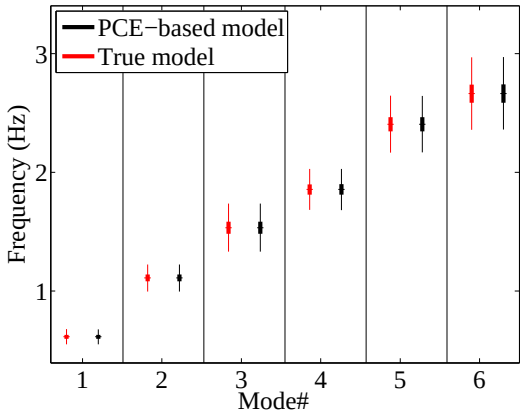

(b) Eigenfrequencies

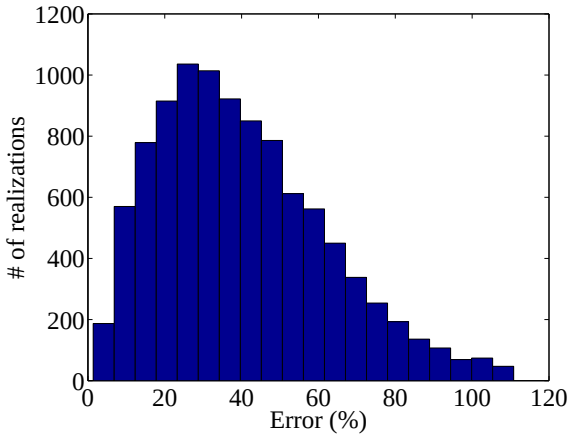

(c) Error analysis of the FRFs

Figure 15: System property comparison between the PCE-based model and the true model obtained over 10,000 points sampled from the parameter space

Moreover, in order to assess the error quantitatively, FRFs of the PCE-based models have been calculated and compared with the corresponding true model in the root-mean-square sense. This error is evaluated using Eq. (43), its average over the outputs is presented in Fig. 15c. Since this result could be misleading, two cases are chosen to further elaborate: one case with an average error, about 40%, and one with the maximum error, about 110% , which are shown respectively in Figs. 16 and 17 for the first output. In each figure, two plots are shown: one for the case that PCE is used for predicting the full model, Figs. 16a and 17a , and one for the reduced model, Figs. 16b and 17b.

In both cases, in spite of the large error values, one can observe that the proposed method predicted the full model and the reduced model with excellent accuracy. By scrutinizing the responses around the last two peaks, the source of these large errors is found to be the error in the amplitude of the FRFs close to the eigenfrequencies. Absolute difference between the responses shown by dotted lines in Figs. 16 and 17 confirm this reasoning.

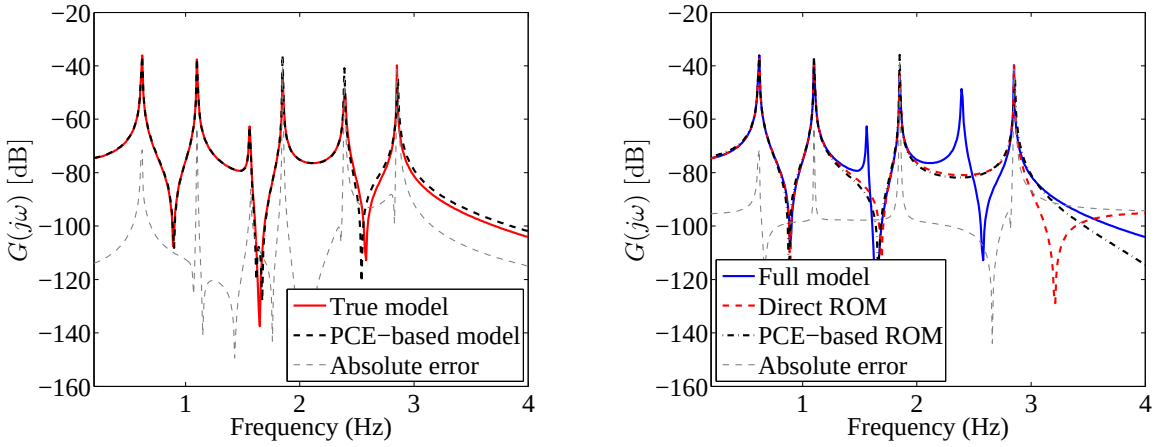

(a) FRF of the full system

(b) FRF of the reduced system

Figure 16: Typical FRF prediction at first system output, FRF of the true (in red) and PCE-based (in black) system and their differences (in dotted line).

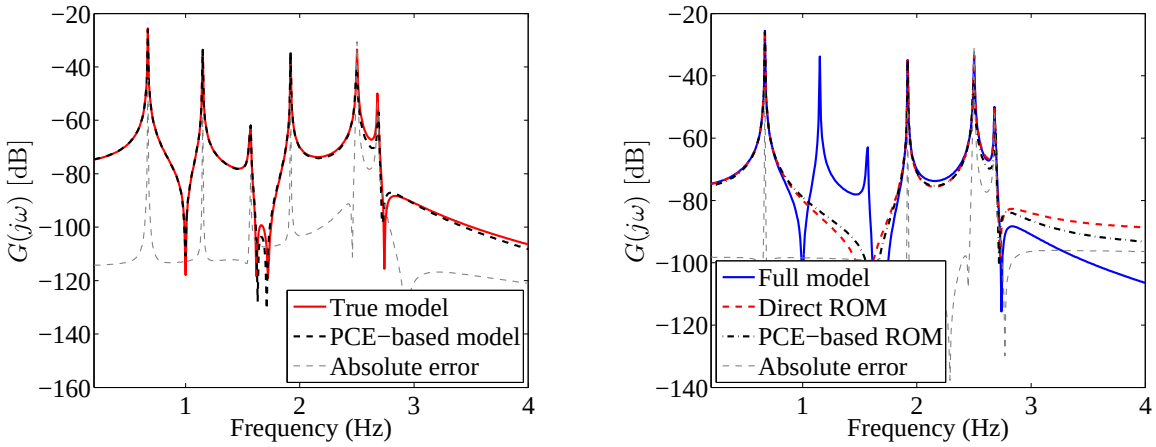

(a) FRF of the full system

(b) FRF of the reduced system

Figure 17: Worst case FRF prediction among 10,000 sample points at first system output, FRF of the true (in red) and PCE-based (in black) system and their differences (in dotted line).

At the end, it should be mentioned that the results indicate excellent accuracy of the proposed method in (*i*) predicting the modal contribution and therefore, right selection of the dominant modes, (*ii*) predicting the full model as well as the reduced model for a case with high-dimensional parameter space.

5.5 3D Timoshenko beam: large-scale problem

The last example is selected to demonstrate the application of the proposed method to a large-scale system. The system, shown in Fig. 18, is a 3D cantilever Timoshenko beam which

is generated in Matlab according to Panzer et al. (2009). This system is similar to the one studied in Panzer et al. (2010). It consists of 100 nodes along the beam, each with 6 degrees of freedom. This results in an LTI system with an order of $N = 1200$ that we want to reduce the system order to $n = 20$. The parameters of the beam are modeled by lognormally distributed random variables with mean values listed in Table 5 and uncertainty of COV = 10%. The damping matrix is $\boldsymbol{V} = C_M\boldsymbol{M} + C_K\boldsymbol{K}$ with $C_M = 8\ s^{-1}$ and $C_K = 8 \times 10^{-6}\ s$. The system has one input force at the free end of the beam and 6 system outputs equidistantly located along the beam, shown by the black circles. In order to perform the accuracy analysis, FRF of the system is evaluated at a frequency range from 1 to 5000 Hz.

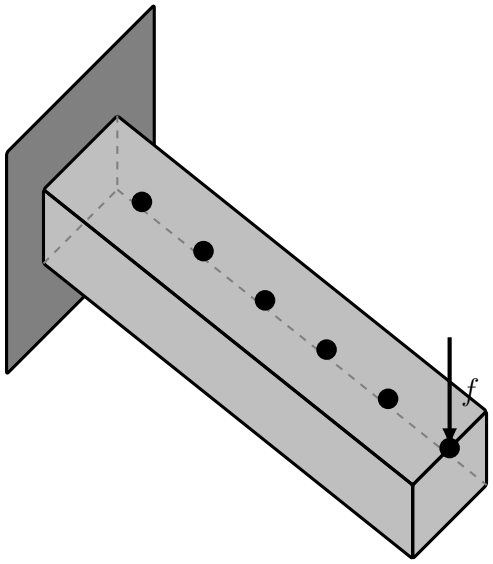

Figure 18: 3D cantilever Timoshenko beam

Table 5: The variables of the 3D Timoshenko beam

Variables	Length (l)	Thickness (t)	Height (h)	Density (ρ)	Young's modulus (E)	Poisson's ratio (ν)
Unit	$[m]$	$[m]$	$[m]$	$[kg/m^3]$	$[GPa]$	
Mean	1	0.01	0.01	7850	210	0.3
COV (%)	10	10	10	10	10	10

50 points sampled from the parameter space using Sobol sampling method constitute the ED. In this case, since the order of the full model is so large, making PCE for all the system matrices is not feasible, therefore the model order should be reduced to a smaller order, *e.g.* $n_{temp} = 40$, before calculating the PCE. Through this example, in order to distinguish the reduction step before and after making PCE, they will be denoted by *pre-* and *post*-PCE reduction, respectively. The LAR algorithm has been employed to build sparse PCEs with

adaptive degree. PCA has been performed over the $\boldsymbol{C}$ matrix and the dominant components are selected such that $\sum_{i=1}^{\hat{N}_Y} \lambda_i^{COV} = 0.99 \sum_{i=1}^{N_Y} \lambda_i^{COV}$ here λ^{COV} are the eigenvalues of the covariance matrix, see Eq. (15). This truncation reduced the number of random outputs from 240×2 to 6 components.

10,000 points sampled from the parameter space by using Monte-Carlo sampling as the validation points and both the true and the PCE-based models are evaluated at these points. Their associated FRFs are calculated and compared by using Eq. (43). The mean value of the obtained errors over the outputs, shown in Fig. 19, demonstrates the accuracy of the method in predicting the FRFs.

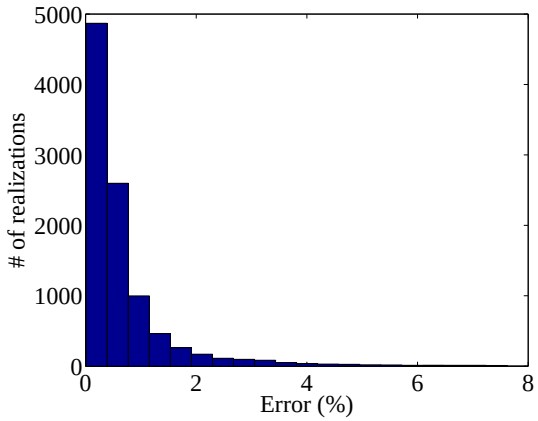

Figure 19: Error analysis of the FRFs of the post-PCE reduced order model in comparison with the true model evaluated by Eq. (43), averaged over the outputs.

As an individual system comparison, a case with the maximum error, about 7% , is considered. Fig. 20. illustrates the comparison between the FRFs of the PCE-based model and the true model in pre- and post-PCE reduction. Spectrum of the eigenvalues for the models with different orders are also shown in Fig. 21. Accuracy of the method in predicting the PCE-based ROM for large-scale systems can be simply inferred.

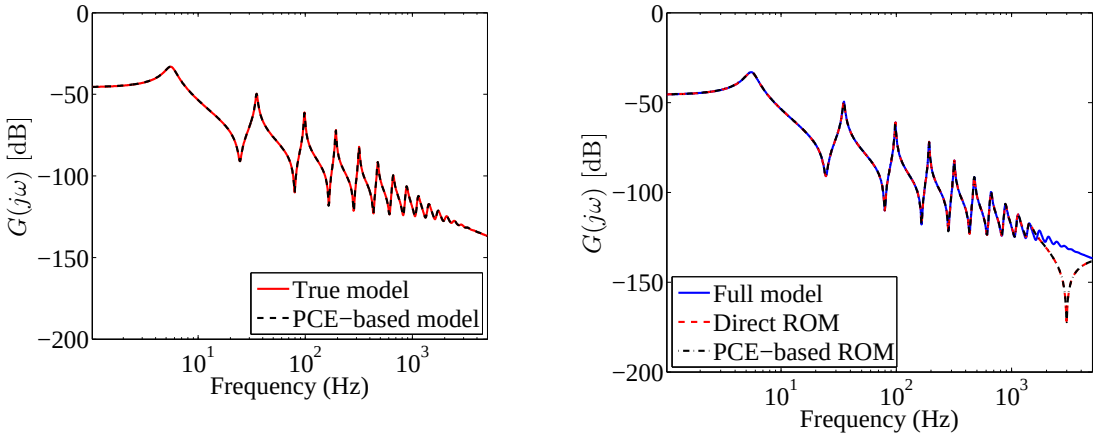

(a) FRF of the full system

(b) FRF of the reduced system

Figure 20: Worst case FRF prediction among 10,000 sample points at first system output, evaluated by true model (in red) and PCE-based model (in black).

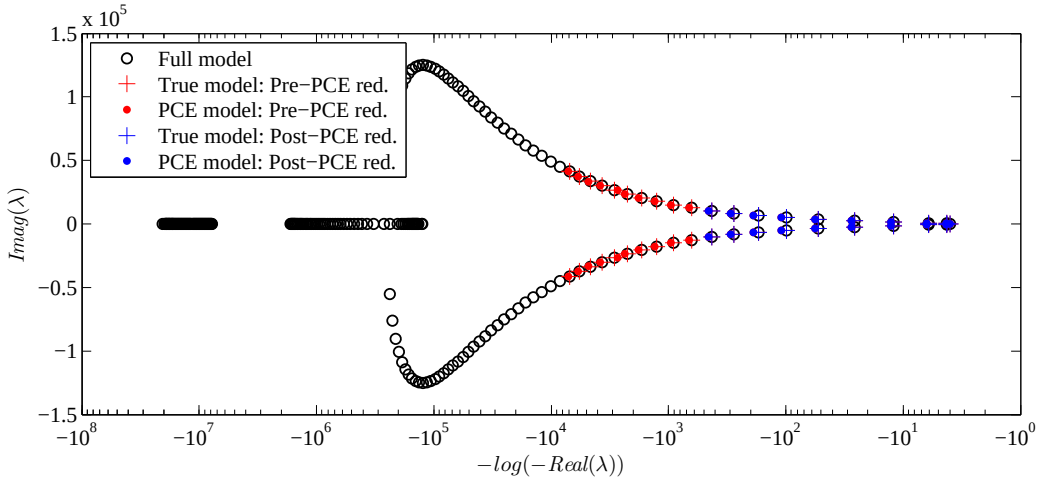

Figure 21: Eigenvalue spectrum of the systems realized at the parameter set with the maximum average error.

6 Concluding remarks

In this paper, a PCE-based parametric model reduction method for dynamic systems has been developed. This method consists of a PCE-based surrogate model for state-space models together with a PCE-based modal dominancy method to reduce the model order, if required. For this purpose, a method has been proposed based on QR factorization to fix the eigenvectors of the modes with coalescent eigenvalues. Moreover, a new correlation metric has been introduced for mode tracking, which was shown to be effective to resolve the spatial aliasing phenomenon in cases with few number of sensors. The problem of the curse of dimensionality

of PCEs in cases with large parameter spaces was alleviated by employing the LAR algorithm to build sparse PCEs together with an adaptive degree strategies. In order to reduce the number of random outputs in large-scale systems with high model orders two solutions were proposed: first, reduce the model order to an intermediate level before making PCE and second, use of PCA while making PCE. Successful application of the proposed method to four case studies indicate its capability in accurately predicting the modal contributions, eigenvalues, and more importantly, full and reduced order systems. The case studies are selected such that each of them resembles a frequently occurred challenge in complex systems, such as mode veering, large parameter space and large-scale systems.

Acknowledgments

The authors would like to appreciate financial support from *Iran National Elite Foundation*.

References

Allemang, R. J. (2003). The modal assurance criterion–twenty years of use and abuse. *Sound vibration 37*(8), 14–23.

Amsallem, D. and C. Farhat (2008). Interpolation method for adapting reduced-order models and application to aeroelasticity. *AIAA journal 46*, 1803–1813.

Amsallem, D. and C. Farhat (2011). An online method for interpolating linear parametric reduced-order models. *SIAM J. Sci. Comput. 33*, 2169–2198.

Antoulas, A. C. (2005). *Approximation of large-scale dynamical systems*, Volume 6. Siam.

Antoulas, A. C., D. C. Sorensen, and S. Gugercin (2001). A survey of model reduction methods for large-scale systems. *Contemporary mathematics 280*, 193–220.

Avitabile, P. and J. O'Callahan (2009). Efficient techniques for forced response involving linear modal components interconnected by discrete nonlinear connection elements. *Mech. Syst. Signal Pr. 23*, 45–67.

Baur, U., P. Benner, A. Greiner, J. G. Korvink, J. Lienemann, and C. Moosmann (2011). Parameter preserving model order reduction for MEMS applications. *Math. Comp. Model Dyn. 17*, 297–317.

Benner, P., S. Gugercin, and K. Willcox (2013). A survey of model reduction methods for parametric systems.

Berveiller, M., B. Sudret, and M. Lemaire (2006). Stochastic finite element: a non intrusive approach by regression. *Eur. J. Comput. Mech. 15*, 81–92.

Blatman, G. and B. Sudret (2008). Sparse polynomial chaos expansions and adaptive stochastic finite elements using a regression approach. *Comptes Rendus Mécanique 336*, 518–523.

Blatman, G. and B. Sudret (2010). An adaptive algorithm to build up sparse polynomial chaos expansions for stochastic finite element analysis. *Probabilist. Eng. Mech. 25*, 183–197.

Blatman, G. and B. Sudret (2011). Adaptive sparse polynomial chaos expansion based on least angle regression. *J. Comput. Phys. 230*, 2345–2367.

Blatman, G. and B. Sudret (2013). Sparse polynomial chaos expansions of vector-valued response quantities. In G. Deodatis (Ed.), *Proc. 11th Int. Conf. Struct. Safety and Reliability (ICOSSAR'2013), New York, USA*.

Bogoevska, S., M. Spiridonakos, E. Chatzi, E. Dumova-Jovanoska, and R. Höffer (2017). A data-driven diagnostic framework for wind turbine structures: A holistic approach. *Sensors 17*, 720.

Dertimanis, V., M. Spiridonakos, and E. Chatzi (2017). Data-driven uncertainty quantification of structural systems via b-spline expansion. *Computers & Structures*.

Efron, B., T. Hastie, I. Johnstone, R. Tibshirani, et al. (2004). Least angle regression. *Ann. Stat. 32*, 407–499.

Frangos, M., Y. Marzouk, K. Willcox, and B. van Bloemen Waanders (2010). Surrogate and reduced-order modeling: A comparison of approaches for large-scale statistical inverse problems. *Large-Scale Inverse Problems and Quantification of Uncertainty 123149*.

Fricker, T. E., J. E. Oakley, N. D. Sims, and K. Worden (2011). Probabilistic uncertainty analysis of an FRF of a structure using a Gaussian process emulator. *Mech. Syst. Signal Pr. 25*, 2962–2975.

Ghanem, R. and D. Ghiocel (1998). Stochastic seismic soil-structure interaction using the homogeneous chaos expansion. In *Proc. 12th ASCE Engineering Mechanics Division Conference, La Jolla, California, USA*.

Ghanem, R. G. and P. D. Spanos (2003). *Stochastic finite elements: a spectral approach*. Courier Corporation.

Ghiocel, D. and R. Ghanem (2002). Stochastic finite element analysis of seismic soil-structure interaction. *J. Eng. Mech. 128*, 66–77.

Gilli, L., D. Lathouwers, J. Kloosterman, T. van der Hagen, A. Koning, and D. Rochman (2013). Uncertainty quantification for criticality problems using non-intrusive and adaptive polynomial chaos techniques. *Ann. Nucl. Energy 56*, 71–80.

Hastie, T., J. Taylor, R. Tibshirani, G. Walther, et al. (2007). Forward stagewise regression and the monotone lasso. *Electron. J. Stat. 1*, 1–29.

Jones, D. R., M. Schonlau, and W. J. Welch (1998). Efficient global optimization of expensive black-box functions. *J. Global Optim. 13*, 455–492.

Kersaudy, P., B. Sudret, N. Varsier, O. Picon, and J. Wiart (2015). A new surrogate modeling technique combining Kriging and polynomial chaos expansions–application to uncertainty analysis in computational dosimetry. *J. Comput. Phys. 286*, 103–117.

Kim, T. (2015). Surrogate model reduction for linear dynamic systems based on a frequency domain modal analysis. *Comput. Mech. 56*, 709–723.

Kim, T. (2016). Parametric model reduction for aeroelastic systems: Invariant aeroelastic modes. *J. Fluid Struct. 65*, 196–216.

Kim, T. S. and Y. Y. Kim (2000). MAC-based mode-tracking in structural topology optimization. *Comput Struct 74*, 375–383.

Knio, O. M., H. N. Najm, R. G. Ghanem, et al. (2001). A stochastic projection method for fluid flow: I. basic formulation. *J. Comput. Phys. 173*, 481–511.

Laub, A. J. (2005). *Matrix analysis for scientists and engineers*. Philadelphia, PA, USA: SIAM.

Liu, T., C. Zhao, Q. Li, and L. Zhang (2012). An efficient backward Euler time-integration method for nonlinear dynamic analysis of structures. *Comput. Struct. 106*, 20–28.

Lohmann, B. and R. Eid (2007). Efficient order reduction of parametric and nonlinear models by superposition of locally reduced models. In *Methoden und Anwendungen der Regelungstechnik. Erlangen-Münchener Workshops*, pp. 27–36.

Mai, C., M. Spiridonakos, E. Chatzi, and B. Sudret (2016). Surrogate modelling for stochastic dynamical systems by combining nonlinear autoregressive with exogenous input models and polynomial chaos expansions. *Int. J Uncertain Quantif 6*.

Manan, A. and J. Cooper (2010). Prediction of uncertain frequency response function bounds using polynomial chaos expansion. *J. Sound Vib. 329*, 3348–3358.

Marelli, S. and B. Sudret (2014). UQLab: a framework for uncertainty quantification in matlab. In *Vulnerability, Uncertainty, and Risk: Quantification, Mitigation, and Management*, pp. 2554–2563.

Marelli, S. and B. Sudret (2015). UQLab user manual–polynomial chaos expansions. Technical report, Report UQLab-V0.9-104, Chair of Risk, Safety & Uncertainty Quantification, ETH Zürich.

Morand, H. and R. Ohayon (1995). Fluid structure interaction. *ZAMM Z. Angew. Math. Mech 76*, 376–376.

Panzer, H., J. Hubele, R. Eid, and B. Lohmann (2009). Generating a parametric finite element model of a 3d cantilever timoshenko beam using matlab. *Tech. reports on aut. control, Inst. Aut. Control, TU München*.

Panzer, H., J. Mohring, R. Eid, and B. Lohmann (2010). Parametric model order reduction by matrix interpolation. *at-Automatisierungstechnik 58*, 475–484.

Rahrovani, S., M. K. Vakilzadeh, and T. Abrahamsson (2014). Modal dominancy analysis based on modal contribution to frequency response function $\mathcal{H}2$-norm. *Mech. Syst. Signal Pr. 48*, 218–231.

Schöbi, R., B. Sudret, and J. Wiart (2015). Polynomial-chaos-based Kriging. *Int. J. Uncertainty Quantification 5*, 171–193.

Schuëller, G. and H. Pradlwarter (2009). Uncertain linear systems in dynamics: Retrospective and recent developments by stochastic approaches. *Eng. Struct. 31*, 2507–2517.

Sobol, I. (1990). Quasi-monte carlo methods. *Progress in Nuclear Energy 24*, 55–61.

Soize, C. and R. Ghanem (2004). Physical systems with random uncertainties: chaos representations with arbitrary probability measure. *SIAM J. Sci. Comput. 26*, 395–410.

Stephen, N. (2009). On veering of eigenvalue loci. *J. Vib. Acoust. 131*, 054501.

Sudret, B. (2007). Uncertainty propagation and sensitivity analysis in mechanical models – contributions to structural reliability and stochastic spectral methods. Technical report. Habilitation à diriger des recherches, Université Blaise Pascal, Clermont-Ferrand, France (229 pages).

Tak, M. and T. Park (2013). High scalable non-overlapping domain decomposition method using a direct method for finite element analysis. *Comput. Methods Appl. Mech. Engrg. 264*, 108–128.

Wiener, N. (1938). The homogeneous chaos. *Amer. J. Math.*, 897–936.

Xiu, D. and G. E. Karniadakis (2002). The Wiener–Askey polynomial chaos for stochastic differential equations. *SIAM J. Sci. Comput. 24*, 619–644.

Yaghoubi, V. and T. Abrahamsson (2014). The modal observability correlation as a modal correlation metric. In *Topics in Modal Analysis, Volume 7*, pp. 487–494. Springer.

Yaghoubi, V., T. Abrahamsson, and E. A. Johnson (2016). An efficient exponential predictor-corrector time integration method for structures with local nonlinearity. *Eng. Struct. 128*, 344 – 361.

Yaghoubi, V., S. Marelli, B. Sudret, and T. Abrahamsson (2017). Sparse polynomial chaos expansions of frequency response functions using stochastic frequency transformation. *Probab. Eng. Mech. 48*, 39 – 58.

Yaghoubi, V., M. K. Vakilzadeh, and T. Abrahamsson (2015). A parallel solution method for structural dynamic response analysis. In *Dynamics of Coupled Structures, Volume 4*, pp. 149–161. Springer.

Yang, J., B. Faverjon, H. Peters, and N. Kessissoglou (2015). Application of polynomial chaos expansion and model order reduction for dynamic analysis of structures with uncertainties. *Procedia IUTAM 13*, 63–70.